FINAL REPORT

Prospects for Remediation of 1,2,3-Trichloropropane by Natural and Engineered Abiotic Degradation Reactions

SERDP Project ER-1457

AUGUST 2010

Paul G. Tratnyek
Vaishnavi Sarathy
Alexandra J. Salter
James T. Nurmi
Graham O'Brien Johnson
Tanner DeVoe
Priscilla Lee
Oregon Health & Science University

This document has been cleared for public release

SERDP
DOD · EPA · DOE

Abstract

1,2,3-trichloropropane (TCP) is a contaminant of DOD concern mainly due to it use in solvent formulations for paint and varnish removal, cleaning and degreasing, etc. Compared with other chlorinated solvents, TCP is similarly mobile, exceptionally persistent, and relatively toxic, suggesting that TCP will pose clean-up challenges that are similar, but in some respects more difficult. While TCP is characteristically recalcitrant, to both abiotic (and biotic) degradation pathways, potentially beneficial transformations of TCP are possible by hydrolysis, elimination, reduction, and oxidation. The goal of this project was to provide a detailed, quantitative characterization of these pathways of TCP degradation in water or soil.

Hydrolysis of TCP under ambient conditions of pH and temperature is negligible, but base-catalyzed hydrolysis becomes favorable at high pH and temperature, such as under conditions of *in situ* thermal remediation (ISTR). Oxidation of TCP is less favorable than it is with many contaminants and is negligible with mild/specific oxidants like permanganate. However, the stronger oxidants involved in some *in situ* chemical oxidation (ISCO) processes—esp. hydroxyl and sulfate radicals—do oxidize TCP. Reduction of TCP under the mild conditions involved in natural attenuation is negligible, and the treatments used in conventional forms of in situ chemical reduction (ISCR)—such as granular zero-valent iron (ZVI)—give only slow dechlorination. More rapid degradation of TCP was obtained by reduction with nano ZVI, palladized nano ZVI, and zero-valent zinc (ZVZ). The potential for remediation of TCP with ZVZ was investigated in batch and column experiments because this combination might prove to be a novel solution to a distinctive problem.

Table of Contents

List of Figures

List of Tables

List of Acronyms

AGW	artificial groundwater
AGWP	artificial groundwater from site "P"
CoC	contaminant of concern
CP	chronopotentiometry
1,1-DCA	1,1-dichloroethane
1,2-DCA	1,2-dichloroethane
DCP	1,2-dichloropropane
DI	deionized
DO/DI	deoxygenated, deionized
ECD	electron capture detector
E_{corr}	corrosion potential
EDTA	ethylenediaminetetraacetic acid
ERIS	(Army) Environmental Restoration Information System
ERPIMS	(Air Force) Environmental Restoration Program Information Management System
$Fe^{H2(D)}$	Toda RNIP-10DS, dry
Fe^{HSA}	Hepure "High Sulfur Atomized" Iron
FID	flame ionization detector
GC	gas chromatography
ISCO	*in-situ* chemical oxidation
ISTR	*in-situ* thermal reduction
k_M	mass-normalized reaction rate
k_{obs}	observed reaction rate
k_{SA}	surface-area-normalized reaction rate
LSV	linear sweep voltammograms
MCL	mean contaminant level
MS	mass spectrometry
NIOSH	National Institute for Occupational Safety and Health
NORM	(Navy) Normalized Database
nZVI	nano zero-valent iron
nZVZ	nano zero-valent zinc
QMP	Quebec Metal Products

QSAR	quantitative structure-activity relationship
RfD	reference dose
RNO	p-nitroso dimethylanaline
SWP	site water "P"
TCA	trichloroethane
TCE	tetrachloroethylene
TCP	1,2,3-trichloropropane
ZVI	zero-valent iron
ZVZ	zero-valent zinc

Background

Statement of the Problem

1,2,3-Trichloropropane (TCP) has been used in a variety of chemical production processes and agricultural chemicals including widely used soil fumigants. The primary cause for concern at contaminated sites is spills associated with its use as a solvent (paint and varnish removal, cleaning and degreasing, etc.). TCP has been detected in more than three hundred drinking water wells in California (http://www.cdph.ca.gov/certlic/ drinkingwater/Pages/123TCP.aspx). Despite TCP's relatively widespread use, very little data is available on its occurrence in the environment, and few studies have addressed its environmental fate or potential methods for its remediation. The chemical properties and available toxicity data (*1*) suggest that sites where contamination by TCP is significant will pose challenges for clean-up that are at least as severe as those associated with other dense chlorinated solvents.

Currently, there are no state or federal maximum contaminant levels (MCL) defined for TCP. The EPA does, however, have a reference dose (RfD) of 0.006 mg/kg-day, based on a non-cancer endpoint (http://www.epa.gov/ncea/iris/subst/0200.htm), and TCP has been designated as "reasonably anticipated to be a human carcinogen" (*2*). Among other advisories, NIOSH considers TCP as a potential occupational carcinogen, and has set recommended exposure levels (REL) at 10 ppm (http://www.cdc.gov/niosh/docs/81-123/). NIOSH also considers 100 ppm of TCP in air to be an immediate danger to life and health. California has currently set their notification (action or reporting) levels by the most precautionary criteria. The California Department of Public Health has a notification level of 0.005 ppb for TCP in drinking water, which is much lower than the corresponding level for TCA (trichloroethane) or TCE (trichloroethene).

Although 1,2,3-trichloropropane (TCP) has been used in a variety of chemical production processes and agricultural chemicals, the primary cause for concern at DoD sites is spills associated with its use as a solvent (paint and varnish removal, cleaning and degreasing, etc.). Currently, the frequency and severity of sites contaminated in this way is not well characterized: although we have obtained a summary of occurrence data from the Army (ERIS), Navy (NORM), and Air Force (ERPIMS) databases, few if any of the sites were actively monitoring for TCP. If the regulatory environment for TCP changes, it is likely that detections will be reported more frequently. Therefore, a better understanding of the fate of TCP, and options for its remediation, is needed.

Project Goals and Objectives

The goal of this project is to determine the rates and products of TCP degradation by all of the major types of chemical reactions that are relevant to natural and engineered

strategies for in situ remediation—including hydrolysis, elimination, reduction, and oxidation—over the full range of conditions that are relevant to groundwater. The original project was organization into objectives and tasks is shown in Table 1.

Table 1. Summary of the Original Technical Objectives and Tasks

Objective 1—Analytical Method
• Task 1.1. Develop analytical method based on GC w/ ECD or MS
Objective 2—Homogeneous Solutions
• Task 2.1. Kinetics/Products of hydrolysis in aqueous buffers
• Task 2.2. Kinetics/Products of substitution/elimination in aqueous sulfide
• Task 2.3. Kinetics/Products of all homogeneous pathways in groundwater
Objective 3—Heterogeneous Reductants
• Task 3.1. Kinetics/Products of reduction by conventional Fe^0
• Task 3.2. Kinetics/Products of reduction by nano Fe^0 and Zn
• Task 3.3. Kinetics/Products of reduction by bimetallic Fe^0
• Task 3.4. Kinetics/Products of reduction by Fe_3O_4 w/, w/o Fe^{2+}(ads)
• Task 3.5. Kinetics/Products of reduction by Fe_2O_3 with Fe^{2+}(ads)
• Task 3.6. Kinetics/Products of reduction by FeS
Objective 4—Homogeneous Oxidants
• Task 4.1. Kinetics/Products of oxidation by H_2O_2 w/ Fe^{2+} or Fe^0
• Task 4.2. Kinetics/Products of oxidation by O_3 w/, w/o H_2O_2
• Task 4.3. Kinetics/Products of oxidation by Persulfate (w/, w/o heat)
• Task 4.4. Kinetics/Products of oxidation by Permanganate

The timeline for addressing the tasks given in Table 1, from the original design of this project, is summarized in Table 2. The first group of tasks (analytical methods) was done in the first year. Little work was done that year on the second and third groups of tasks but we completed much of the work the fourth group of tasks (homogeneous oxidants). In the 2nd year, we accomplished much of what was proposed on the second and third groups of tasks. In the third year, we continued to focus mostly on heterogeneous reductants (as recommended by during the last IPR for this project).

Table 2. Original Timeline with Categories of Tasks.

	Project Year 1				Project Year II				Project Year III			
Group/Tasks	1/4	2/4	3/4	4/4	1/4	2/4	3/4	4/4	1/4	2/4	3/4	4/4

Analytical Methods										
Homogeneous Solutions										
Heterogeneous Reductants										
Homogeneous Oxidants										

Of the few promising options for remediation of TCP contaminated groundwater that we identified during the first two years of the project, the one that has attracted the most interest is zero-valent zinc (ZVZ). Preliminary results in PY 2 indicated that ZVZ degrades TCP more rapidly than other reductants (e.g., zero-valent iron, ZVI) and appears to give complete dechlorination (to propanes and propenes). The limited amount of prior work on contaminant reduction by ZVZ was focused on chlorinated ethenes and methanes, so it missed what we now recognize to be the biggest advantage of ZVZ (better degradation of primary chlorinated ethanes and propanes). Because of this, it appears that there has been little attention given to the suitability of ZVZ for water treatment applications.

Investigation of this, and in particular the treatment of TCP contaminated groundwater with ZVZ, seemed like a natural extension of the work that was originally funded under ER-1457. We proposed to do this work as a 4th year of the current project through a whitepaper to SERDP titled "Reduction of 1,2,3-trichloropropane (TCP) with zero-valent zinc". The extension was approved, with the following tasks:

Table 3. Summary of Year IV Scope and Objectives

Objective A—Optimize Selection of ZVZ
• *Task A1.* Screen a variety of ZVZ containing granular materials for reactivity with TCP, focusing on products that are commercially available or otherwise promising for full-scale applications.
• *Task A2.* Synthesize (or acquire) nanosized ZVZ (nZVZ) and characterize its reactivity with TCP.
• *Task A3.* Prepare and test bimetallic core/shell nanoparticles with (*i*) base metal core and shell (e.g., Fe^0/Zn^0 and Zn^0/Fe^0 to test for Galvanic coupling effects on contaminant degradation) and (*ii*) base metal core with noble metal shell (e.g., Zn^0/Pd^0, to test for catalytic hydrogenation of contaminants).
• *Task A4.* Prepare and test inter-metallic effects using alloys of Fe^0 and Zn^0.
Objective B—Optimization of the ZVZ Process for TCP
• *Task B1.* Measure the kinetics and products of TCP in short term batch experiments done with artificial groundwater with a range of chemistries
• *Task B2.* Measure the kinetics and products of TCP in long-term batch experiments done with respikes of TCP
• *Task B3.* Measure the kinetics and products of TCP in medium-term (e.g.

Objective C—Assessing Implications for Water Chemistry and Permeability
• *Task C1.* Run columns with various ratios of ZVZ and sand until pH and dissolved Zn^{2+} reach steady-state. Then vary flow rate, and feed water chemistry (pH, NOM concentration, TCP concentration) and record any perturbations in effluent chemistry and pressure drop.
• *Task C2.* Using the results of Task C1 to select an optimal ratio of ZVZ to sand, prepare columns with a ZVZ containing zone between zones of sand. Measure pH, Zn^{2+} and TCP concentration along the column length—focusing on the interfaces with the up-gradient and down-gradient sand zones—as the column conditions reach steady state. Then, sacrifice the column and identify the precipitate phases along the length of the column.
• *Task C3.* Perform equilibrium geochemical speciation modeling to aid in interpretation of the data from all of the above tasks.

The timeline for addressing the new tasks given in Table 3 is summarized in Table 4. Some work on this new set of tasks was started toward the end of PY 3, so some of the results are included below (under Task 3.2).

Table 4. Timeline for New PY4 Work.

Group/Tasks	PY1 (1/3)				PYII (2/3)				PYIII (3/3)			
Optimize selection of ZVZ	▓	▓	▓	▓								
Optimize process					▓	▓	▓	▓				
Test site conditions									▓	▓	▓	▓

In addition to this new PY4 work under ER-1457, our PY3 work on degrading TCP with ZVZ has generated interest from site managers and consultants, who have been struggling with some TCP contaminated sites and a lack of any good prospects for remediating it. Two worth noting, even though they are not DOD sites, arose from agriculture operations using TCP containing (or contaminated) formulations of soil fumigants. One of these sites has begun pilot testing of an above ground treatment systems using ZVZ based on the results of our work.

In addition, one DOD site—Camp Pendleton—emerged as a leading candidate for testing the field scale feasibility of using ZVZ to remove TCP from groundwater. In 2008, a proposal was prepared and funded by the Navy Environmental Sustainability Development to Integration (NESDI) Program (PI: Nancy Ruiz). The NESDI project is focused on meeting the Navy's short- to medium-term need to treat the TCP contaminated groundwater at Camp Pendleton in order to continue to use existing drinking water wells. The goal was to demonstrate that TCP can be removed from water pumped from wells at the site using above ground canisters packed with ZVZ (and/or

Fe[HSA], defined below). With this approach, we believe it will be possible to decrease TCP concentrations to below the California action level of 0.005 ppb, with the main products being fully dechlorinated propenes and propanes, with no detectable chlorinated hydrocarbon residuals. This level of system performance required optimization for the conditions at Camp Pendleton, so we conducted some preliminary testing with site water in batch-reactor experiments and bench-scale laboratory columns as part of the extension of the current SERDP project. Currently, the materials and parameters selected through our preliminary tests are being evaluated in long-term *ex situ* columns at Camp Pendleton for future us in *in situ* PRB or *ex situ* point of use drinking water treatment for TCP-impacted groundwater.

Results

For the purposes of this report, we have organized our results in a manner that roughly follows the tasks and timeline of the original project proposal. The section breaks and headings also reflect how the project results were grouped into manuscripts for publication. In each case, the anticipated publications are identified in a footnote to the section heading. Details on our publications are given below as footnotes to the corresponding sections on results. A number of presentations on this work were given that cover most of the scope of this project, and these are listed in an appendix.

General Analytical Methods

Task 1.1. Gas Chromatography Methods

In order to be able to move efficiently through the degradation studies, we needed reliable methods for routine analysis of 1,2,3-TCP and most of its degradation products. The variety of anticipated degradation products are summarized in Figure 1.
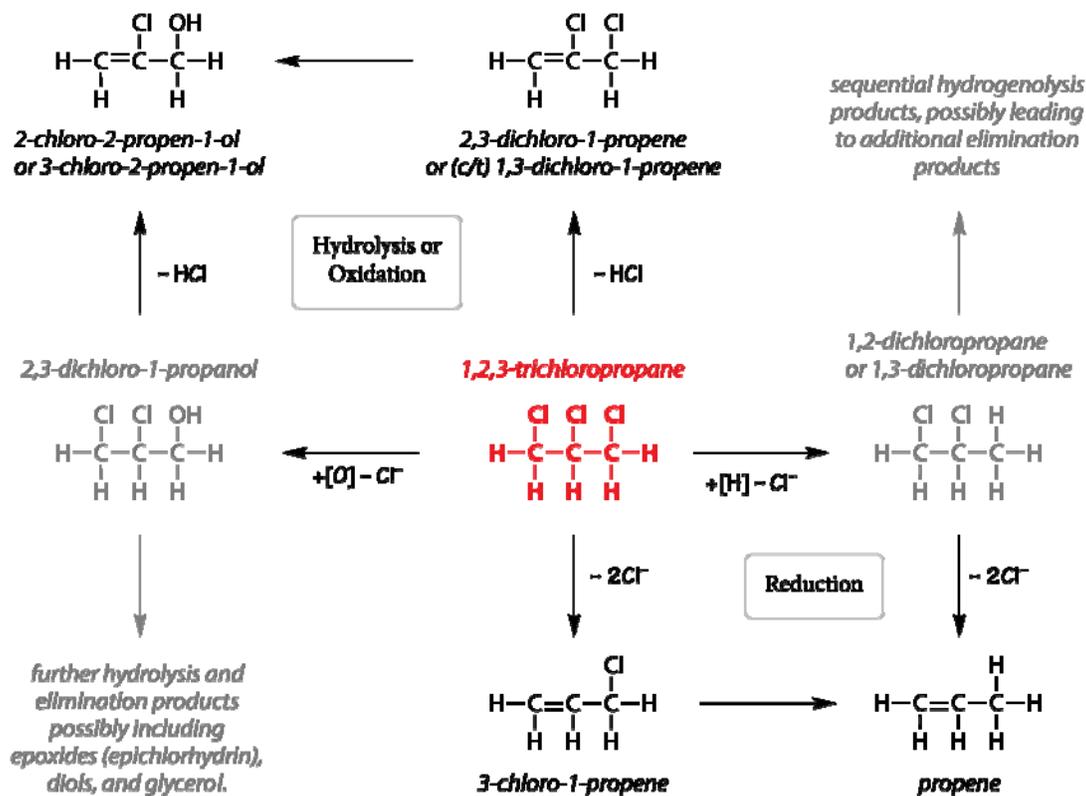
Figure 1. Summary of anticipated, primary reaction pathways for degradation of TCP. Oxidation, hydrolysis, and hydrogenolysis are represented by the horizontal arrows. Elimination (dehydrochlorination) and reductive elimination (reductive β-elimination) are shown with vertical arrows. [O] represents oxygenation (by oxidation or hydrolysis), [H] represents reduction. Gray indicates products that are likely to be of lesser significance. Based on (*3, 4*).

Early in the project, we settled on gas chromatography with electron capture detection (GC/ECD) for detection of TCP, and flame ionization detection (FID) or mass spectrometry (MS) for the lesser chlorinated by-products.

Details of the GC method we currently use for routine measurement of TCP concentrations are as follows: *Instrument*: HP 5890 Series II gas fitted with an HP 7694 headspace autosampler, an on-column injection port and an electron capture detector, with Peak Simple software. For detection of volatile byproducts along with TCP, we used a manual injection port, with an ECD and FID in series. *Column*: DB-624, 30 m x 0.53 mm i.d. x 3 um film thickness. *Conditions*: Injection port temperature 150 C and detector temperature 300 C for ECD and 350 C for FID. In the autosampler, 10 mL aqueous samples in 20 mL headspace autosampler vials were used.

The only time-consuming part of the method development was locating and identifying products peaks, for which we used both gas chromatography-mass

spectrometry (GC/MS) and comparison to standards obtained from reliable sources. A example, from a batch degradation study of TCP by Fenton reaction, is given as Figure 2.

Figure 2. Sample total ion chromatogram from total GC/MS. Note that Fenton reaction--presumably like other oxidants used in ISCO—degrades TCP to a complex mixture of oxygenated and relatively polar products.

Homogeneous Solutions[1]

Tasks 2.1 to 2.3: DI water, sulfide, and groundwater

Batch experiments were conducted to test for hydrolysis and reduction by sulfide (in homogeneous solution). Site groundwater was not used in this task (but was used in Task 3.2).

Batch reactions for this group of tasks were set up in 40 mL VOA vials capped with *"mini-nert"* septa, fill with deoxygenated MilliQ water (DI). For most hydrolysis experiments, the vials were prepared with 10 mM carbonate buffer, adjusted to pH 11 and 9.2 with 1M HCl. Experiments with sulfide were set up in DI water, with 5 mM Na_2S from a stock of pure Na_2S (solid). The resulting pH was measured to be 11.6, which ensured the sulfide was entirely as bisulfide. Replicates were set up for all experiments. 500 uL of saturated TCP solution was injected in each vial to bring the

---

[1] Our results on hydrolysis were published in Sarathy et al. (*4*).

initial [TCP] to 1.48×10^{-4} M. During sampling, 1 mL of the reaction solution was extracted, and diluted to 10 mL in a 20 mL headspace autosampler vial, and then analyzed via GC-ECD.

Representative results are summarized in Figure 3. TCP losses in the blanks (DI water only) were negligible, and all combinations of replicates gave very good reproducibility. There was no degradation of TCP in pH 9.2 carbonate or in unbuffered DI-water controls ("blank", pH 8). In pH 11 carbonate, however, TCP was degraded with $t_{1/2} = 48$ days. For reasons we describe below, we believe this is due to general-base catalysis, not a specific buffer catalysis effect due to particular carbonate species.
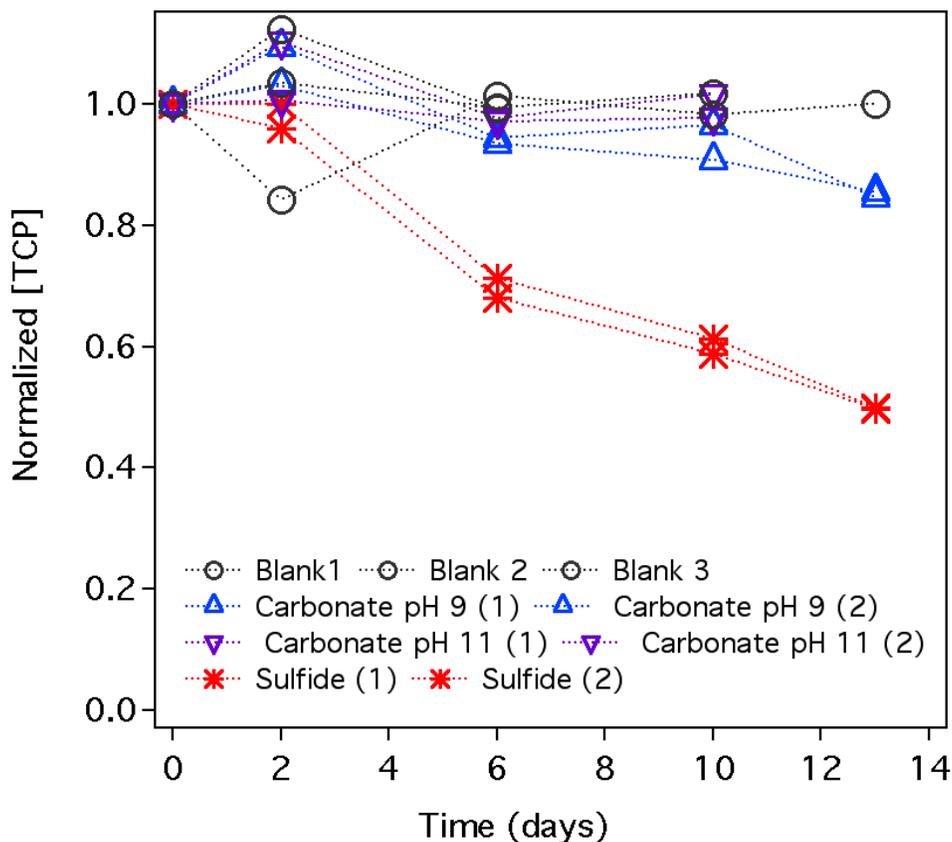
Figure 3. Disappearance kinetics of TCP in homogeneous aqueous solutions, including: DI water controls, carbonate buffered DI water (at pH 9.2 and 11), and 5 mM sulfide (pH 11.6). The numbers 1, 2, and 3 in the caption represent replicates.

Additional experiments were done with 5 mM Na_2S to test for TCP degradation with this nucleophile (Task 2.2), and an example is shown in Figure 3. Under these conditions, fairly rapid degradation ($t_{1/2} = 12$ days) was observed, but this solution had pH 11.6, which would favor base-catalyzed hydrolysis. Without further experiments, we cannot be sure how much of the TCP disappearance under these conditions is due to

nucleophilic attack by hydroxide vs. sulfide. Based on calculations described below, however, we believe the observed degradation is at least in part due to alkaline hydrolysis.

We can put the above results into a modeling context using data from two previously published studies. Ellington (*5*) reported rate constants for both neutral and base-catalyzed TCP degradation in buffered water; Pagan et al. (1998) found that base-catalysis was the only significant pathway for TCP and reported rate constants for it (*6*). In Figure 4, we have used the data from Pagan et al. to calculate isotherms (k_{obs} vs. pH) using the Arrhenius equation, with the effect of temperature on K_w for dissociation of water incorporated using the van't Hoff equation. The numbered points are from Ellington and the lettered points are from our work. In general, the results from all three sources agree well.
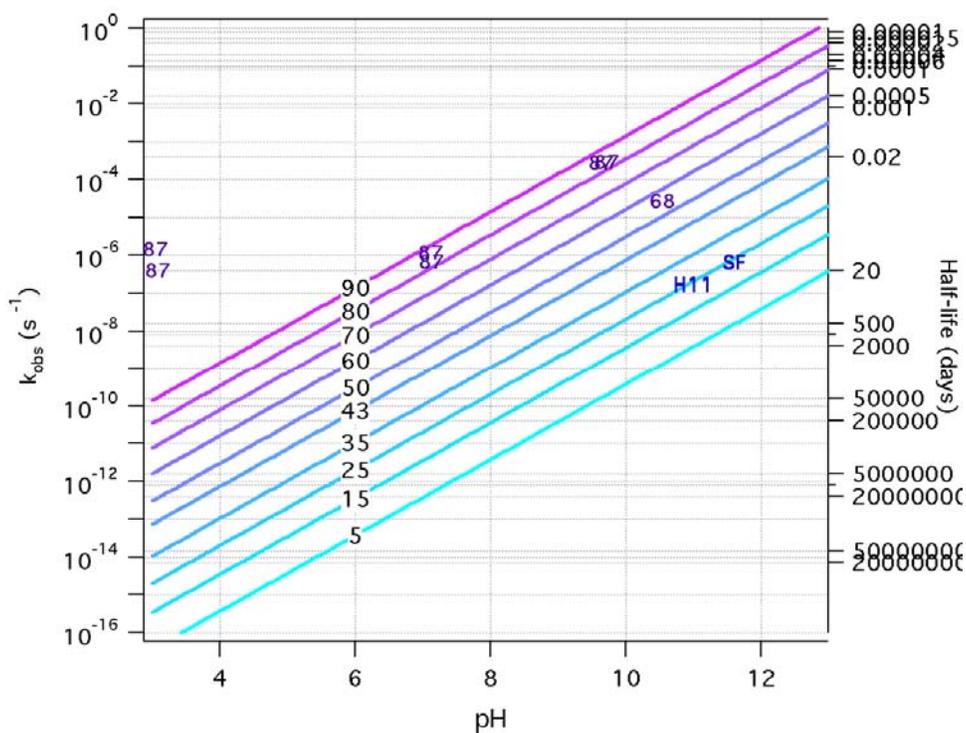
Figure 4. Hydrolysis rate constants vs. pH and temperature calculated from rate constants given in (*6*). Superimposed are individual data points from (*5*) (shown as numbers for their respective temperatures), and our data for pH 11 carbonate buffer (labeled H11), and 5 mM Na_2S at pH = 11.6 (labeled SF).

There is one apparent inconsistency that is revealed by Figure 4, the data from Ellington for 87° C and pH 3 suggest significant hydrolysis by the neutral pathway, but this is not supported by our data or the work by Pagan et al. It is likely this is an error in

the results reported by Ellington, and we currently do not plan to pursue it further. However, it is worth noting here that having reliable data for the rate of TCP hydrolysis is important even if the reactions is slow under most environmentally relevant conditions (see Figure 4, right axis). In particular, those promoting in situ thermal remediation (ISTR), are keen on promoting accelerated hydrolysis of contaminants as one of the benefits of their technology, but they uncertainties in the extrapolation of hydrolysis rate data to high temperatures. Our Figure 4, provides a pretty robust basis for estimating how much hydrolysis of TCP there will be under the conditions of ISTR.

Heterogeneous Reduction Reactions[2]

Tasks 3.1 to 3.3: Fe^0, Bimetallic Fe^0, and Zn

Hydrogenolysis with Zero-Valent Iron

Batch experiments with suspensions of granular Fe^0 have been done using procedures that we have been refining during a decade of work on this system. The details are as follows: In the glove box, 10 mL serum vials containing 1.0 g Fe^0 for the TCP experiments or 1.0, 2.0 were filled with deionized water (leaving no headspace) and crimp sealed with Hycar septa. Spiking with 100 μL aliquots of saturated TCP solution to give initial concentrations of 50-100 μM. Separate vials for each time point were prepared at once, and all vials were mixed together at 40 rpm on a rotator with the plane oriented 85 degrees horizontal. Periodically, vials are sacrificed for analysis by removing the septum and transferring 1 mL for extraction with 1 mL of hexane. The hexane extracts were analyzed by GC as described under Task 1.1.

At first, we surveyed several types of zero-valent iron, with a number of treatments that we though might enhance reactivity against TCP, and the results are summarized in Table 5. The reagent-grade, micron-sized Fe^0 (Fisher electrolytic) was chosen mainly to provide a basis of comparison to other studies. In no case did we see any evidence for reduction (or significant loss by any pathway) of TCP.

Although we did not expect TCP to react rapidly with zero-valent iron (*7-9*), we were somewhat surprised that no reaction was detected because previous work had shown that modest rates of reaction with iron metal were possible. Evidence for the latter is summarized in Figure 5: note that the QSAR predicted value of k_{SA} for TCP is nearly equal to that of TCE; however, the value we estimated from column data in (*10*) is closer to that of vinyl chloride. Clearly, there is a substantial discrepancy to be resolved before we can be sure of the treatability of 1,2,3-TCP with Fe^0.

---

[2] The survey results on reduction, up to our preliminary results with zinc are included in Sarathy et al. (*4*).

Table 5. Results of exploratory experiments with TCP vs. various types of Fe^0.

Iron	Treatment	Length	Result
Micro Fe^0 (PL/CN)	--	--	--
Nano Fe^0 (Toda)	0.005 m^2/mL	1 day	No Rxn
	Sonicate	26 hr	No Rxn
	40ºC	2 days	No Rxn
	pH < 5	1 day	No Rxn
	10 mM H_2O_2	1 day	No Rxn
Bimetallic (Toda)	0.01% Pd	1 day	No Rxn
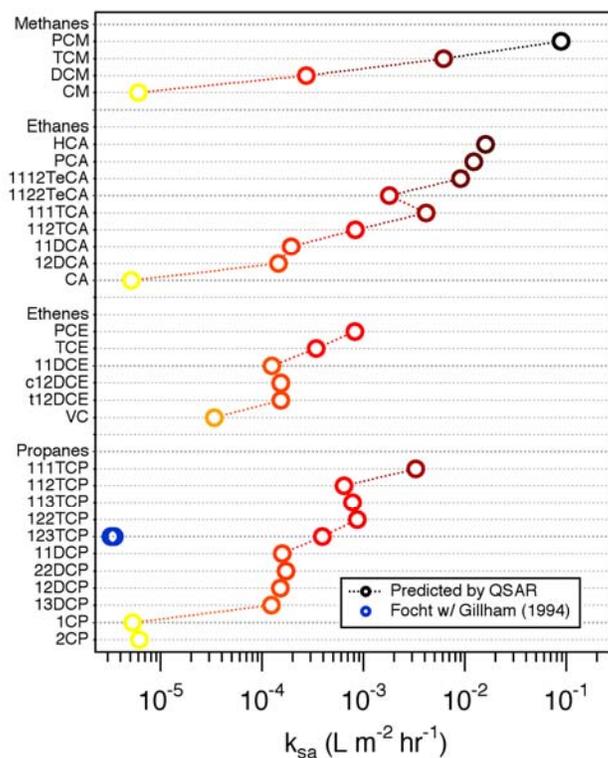
Figure 5. Rate constants (k_{SA}) for degradation of chlorinated methanes, ethanes, ethenes, and propanes by Fe^0. *Yellow to black symbols* represent predicted values calculated from QSARs described in (*8*). *Blue symbols* represent experimental data from (*10*).

The protocol for batch experiments with (conventional) micro- and nano-sized iron was presented in our first annual report. These procedures are essentially identical to those that we have published recently for batch experiments with carbon tetrachloride (*11, 12*). Palladized nano-Fe^0 (Fe^{BH}/Pd) was prepared by Ji-Hun Kim, a visiting scientist from Pohang University of Science and Technology, using an adaptation of the method popularized by Zhang (*13*) (reduction of $FeCl_3$ by sodium borohydride followed by

reaction with palladium acetate). Our batch experiments with the various forms of Fe^0 were executed and analyzed using the same methods as described above.

Our experiments with micron-sized and slurry-aged nano-sized zero valent iron (nZVI) showed no degradation over 30 days (Figure 8). This is less reaction than observed by Focht (*10*) in column experiments with granular ZVI or predictions from QSARs in Scherer et al. (*8*). The inconsistency is significant, so we did few exploratory experiments to see if we could achieve faster degradation by varying conditions that might enhance the reactivity of the iron. We tried adding chloride and aging the iron in water, hoping that these pretreatments would accelerate breakdown of the oxide film on the iron and enhance its reactivity. The results (Figure 8) did not show significant improvements in the reaction rate. We concluded from these experiments that rates of reaction between TCP and regular ZVI will be too slow to of much practical use, and therefore further work on Task 3.1 probably is not necessary.
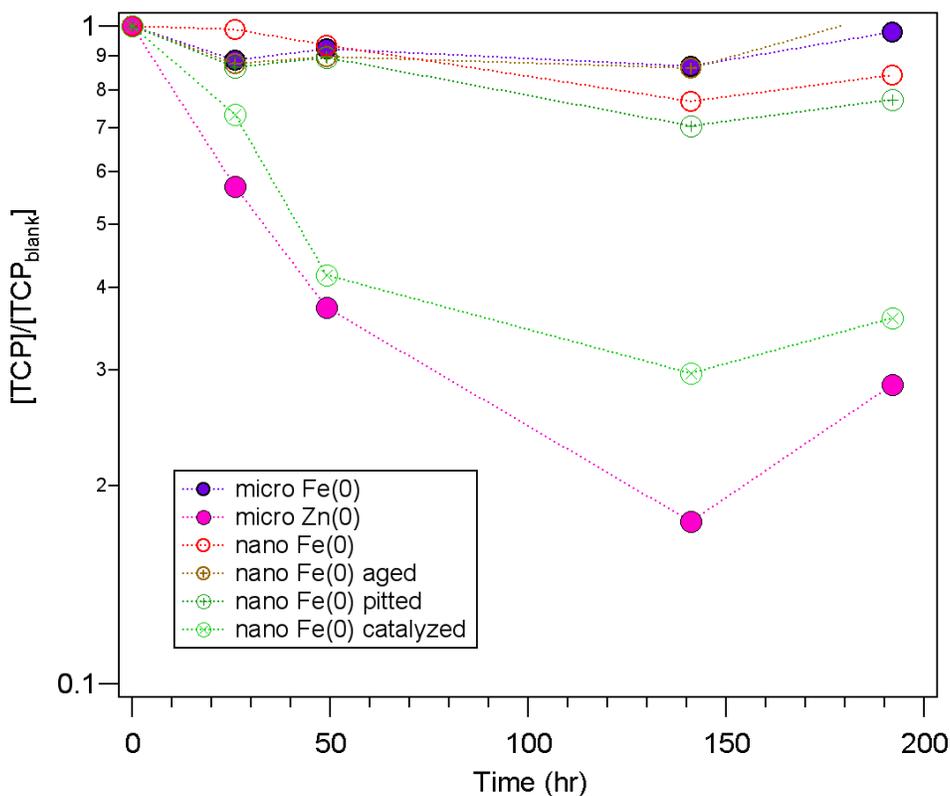
Figure 6. Results of batch experiments done with TCP and a variety of heterogeneous reductant systems. The micro Fe^0 was Fisher electrolytic and the nano Fe^0 was RNIP from Toda. The Zn^0 results are discussed in more detail below. The "Fe^0 catalyzed" experiments where done with RNIP that was modified with covalently bound iron-phthalocynanine.

As a consequence of the above, we have devoted more attention to various "enhanced" varieties of reducing metals (Tasks 3.2-3.3). For example, un-aged nano ZVI from Toda ($Fe^{H2(D)}$, see Sarathy et al. (*12*) for details), which gave reaction rates that were only modestly slower than those observed by Focht. In these experiments, we did not have sufficient degradation of TCP to prove the kinetics in these systems are pseudo first order, but assuming they are—based on all the work done on other chlorinated solvents—we calculated k_{obs} from the data. From k_{obs}, we calculated surface area normalized rate constants (k_{SA}) for comparison among different scenarios. Some of these results are summarized in Figure 7.
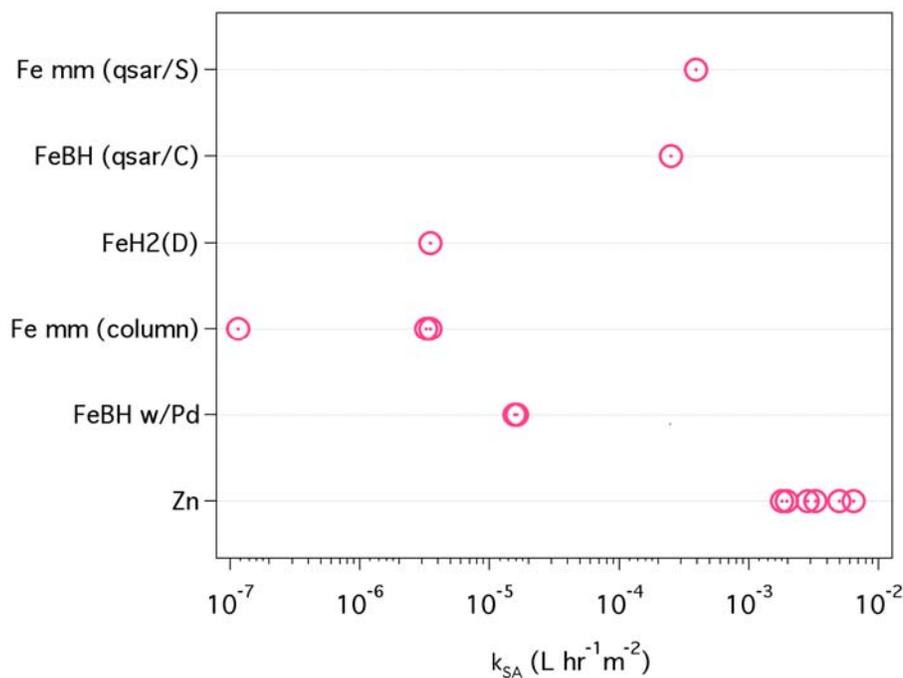
Figure 7. Comparison of estimated and experimental surface area normalized reaction rate constants (k_{SA}) of a variety of reductants with TCP. Fe mm (theor/C) and FeBH (theor/C) refer to values estimated from QSARs for granular mm sized nano-iron (*8*) and borohydride reduced nano-iron (*14*), respectively. Both papers report QSARs for reduction of chlorinated aliphatics using energies of the lowest unoccupied molecular orbital (E_{LUMO}) as the descriptor. The value for $Fe^{H2(D)}$ is for un-aged dry nano-sized zero-valent iron ($Fe^{H2(D)}$), from this study. Fe mm (column) refers to column experiments using granular iron by Focht (*10*). Fe^{BH} w/d Pd refers to the palladized nZVI made by borohydride reduction, by Kim, as described above. The data for granular zinc (Zn) are discussed below.

Although it is natural to assume that the TCP disappearance represented in Figure 7 is do to reduction pathways, most of these systems also cause the pH to increase, and high pH can increases the rate of hydrolysis, as shown in Figure 4. Therefore, it is

possible that some of the disappearance of TCP that we observed is due to hydrolysis not reduction. We cannot evaluate this possibility quantitatively, because we did not measure pHs at the end of all zero-valent iron experiments. However, we can conclude from Figure 4 that the pH would have to be about 11 for hydrolysis to be fast enough to contribute significantly to the degradation of TCP observed with $Fe^{H2(D)}$, or the palladized nZVI, or the zinc. Steady state pHs are not likely to be that high in suspensions of nano-ZVI. Also, we note that the rates of TCP disappearance vary with iron type to a greater degree than the pH is likely to vary.

Our experiments with micron-sized and slurry-aged nano-sized zero valent iron (nZVI)—over a range of conditions—showed little or no degradation over 30 days. We concluded from these experiments that rates of reaction between TCP and regular ZVI will be too slow to of much practical use. However, more promising results were obtained with various "enhanced varieties of reducing metals (Tasks 3.2-3.3). For example, unaged nano ZVI from Toda ($Fe^{H2(D)}$, see Sarathy et al. (12) for details), gave reaction rates that were more substantial. More recently, we have found one type of commercial-grade ZVI that does degrade TCP and significant rates. This material, designated Fe^{HSA} in our work, is "HC-15" from Hepure Technologies (http://www.hepure.com/), which they had provided for testing against other types of ZVI (Peerless, QMP, etc.) with trichloroethylene (TCE). The advantages of Fe^{HSA} are subtle with TCE, but for TCP they are quite dramatic. The results of one experiment are shown in Figure 8. Other experiments have been performed (not shown), with comparable results. The predominant product of this reaction was seen to be propene.

The other two materials included in Figure 8 correspond to palladized ZVI (a result described previously, and a proprietary product made by North American Hoganas and marketed as "Sulfur-Modified Iron". Because of some putative similarities to Fe^{HSA}, we hypothesized that Fe^{SMI} might also show good degradation of TCP. There was little degradation of TCP, however, so we are not testing this material further.

Free Energies of Hydrogenolysis

The slow and sometimes negligible rates of dechlorination of TCP by ZVI can be rationalized theoretical calculations of the free energies of hydrogenolysis for all the congeners of chlorinated propanes. These were calculated for us by Eric Bylaska (Pacific Northwest National Laboratory) using a combination of ab initio quantum mechanical and molecular structure calculation. The methods being used are state-of-the-art, and so the results are as reliable as these types of calculations are likely to be.[3] The results, shown in Figure 9, have been annotated with free energies of dechlorination of the

---

[3] These modeling results are described in Bylaska et al. (15).
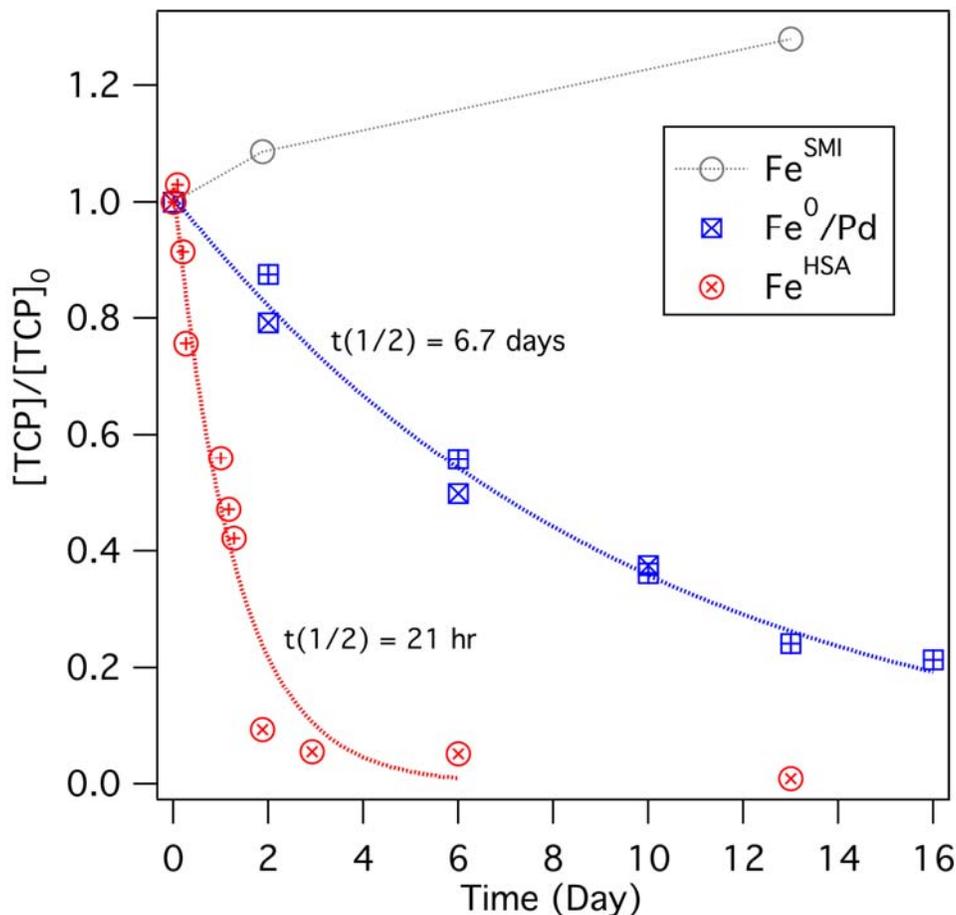
Figure 8. Results of batch experiments done with TCP and several alternative heterogeneous reductants. Fe^{SMI} is SMI-III from North American Hoganas, Fe^{HSA}, is HC-15 from Hepure Technologies, and Fe^0/Pd synthesized at OHSU.

chlorinated methanes (i.e., carbon tetrachloride, chloroform, etc.), which were available from previously performed (unpublished) calculations. The two sets of bars (light and dark blue) are for hydrogenolysis with reductant with standard reduction potentials of -0.8 and -0.92, respectively (both stronger than Fe^{II} but weaker than Fe^0). Clearly, Figure 9 shows that dechlorination of the chlorinated propanes is not very favorable for pathways initiated by concerted dissociative electron transfer (which is assumed to be the rate limiting step and therefore was the focus of these calculations). Dechlorination of the 1,2,3-congener of TCP is less favorable than most of those with more than one chlorine on a carbon.
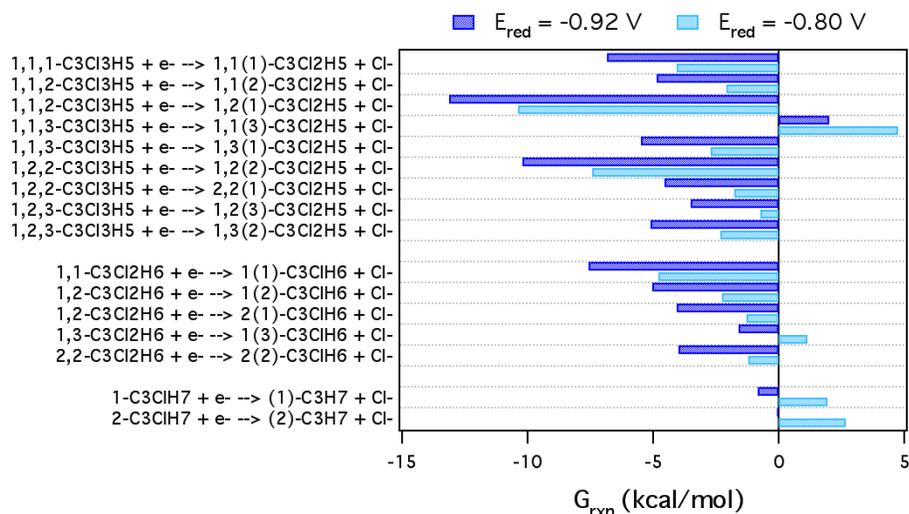
Figure 9. Free energies for dissociative electron transfer (dechlorination) calculated with B3LYP. All chlorinated congeners of propane are included. Two sets of free energies are shown: one for a strong reductant like Fe^0 (with standard reduction potential = -0.92 V) and the other for a more mild reducing agent (with standard reduction potential = -0.80 V) Calculations performed by Eric Bylaska (Pacific Northwest National Laboratory).

Reductive Elimination by Zero-Valent Zinc

Although the results summarized above suggest that dechlorination of TCP initiated by dissociative single-electron transfer (the most likely initial step in hydrogenolysis) is not promising, it is still possible that TCP can be reduced more effectively by reductive (beta) elimination. Zinc metal usually reduces chlorinated hydrocarbons by β-elimination (*16*), and therefore we thought that it might give relatively rapid degradation of TCP. This hypothesis was the academic motivation for us to add experiments with Zn(0) to the scope of this project—which fits pretty well under Tasks 3.2-3.2—however, subsequent developments have made these results look more relevant to real-world remediation applications than we realized. Preliminary results suggested that zinc reacts with TCP quite rapidly.

To follow up on this, five different types of reagent-grade zinc—that varied primarily in size, and in one case, composition—were studied for reactivity with TCP. Most types of zinc were tested both in their native form, and after acid washing. Reactors contained 3 g of Zn and enough deoxygenated MilliQ water to fill the 120 mL serum vial. The vials were crimp-sealed, and let to equilibrate for 24 hours, after which, 1 mL of saturated TCP solution was injected to make initial $[TCP]_{t=0} \approx 10^{-4}$ M. During sampling, 1 mL of the reaction solution was extracted, and diluted to 10 mL in a 20 mL headspace autosampler vial, and then analyzed via GC-ECD. The various treatments and results from this set of experiments are documented in Table 6.

Table 6. Summary of batch experiments with various forms of Zn(0).

No.	Reactant	Media	Mass (g)	Hours Used	Acid-Washed	Rate	SA (m^2/g)	SA (m^2/L)	k_{sa} $(L\ m^{-2}\ hr^{-1})$
1	Zinc, dust, -325 mesh	De-ox DI Water	3	170	No	0.0171	0.350	8.75	0.00195
2	Zinc, dust, -325 mesh	Site-Water	3	244.5	No	0.0008	0.350	8.75	0.00009
3	Zinc, dust, -325 mesh	De-ox DI Water	6	96.5	No	0.0216	0.350	17.50	0.00123
4	"KDF 55" Zinc-Copper Alloy	De-ox DI Water	3	96.75	No	0.0010			
4	Zinc, granular, -10+50 mesh	De-ox DI Water	3	96.75	No	0.0037	0.023	0.58	0.00643
4	Zinc, dust, <10 micron	De-ox DI Water	3	96.75	No	0.0300	0.240	6.00	0.00499
4	Zinc, dust, <10 micron	De-ox DI Water	3	76	No	0.0282	0.240	6.00	0.00470
5	"KDF 55" Zinc-Copper Alloy	De-ox DI Water	3	215	Yes	0.0004			
5	Zinc, granular, -10+50 mesh	De-ox DI Water	3	215	Yes	0.0009	0.020	0.50	0.00180
6	Zinc, granular, 30 mesh	De-ox DI Water	3	191	No	0.0031	0.038	0.95	0.00326
6	Zinc, granular, 30 mesh	De-ox DI Water	3	191	Yes	0.0027	0.038	0.95	0.00284

All of the experiments with Zn^0 and TCP gave pseudo-first-order disappearance kinetics so k_{obs} was calculated, from which we calculated k_{SA}. The k_{obs} data are summarized in Figure 10 (and normalized rate constants are shown in Figure 13). The former shows that the whole range of results with Zn^0 reflect more than an order of magnitude faster TCP degradation than any other treatment. The latter (below), shows substantial variation in the rate of TCP disappearance with the range of zinc types used. The reasons for the differences are not completely clear, but some of the differences certainly are due to surface area. Beyond that, it is notable that the bimetallic combinations with zinc and copper do not appear to offer any advantage.
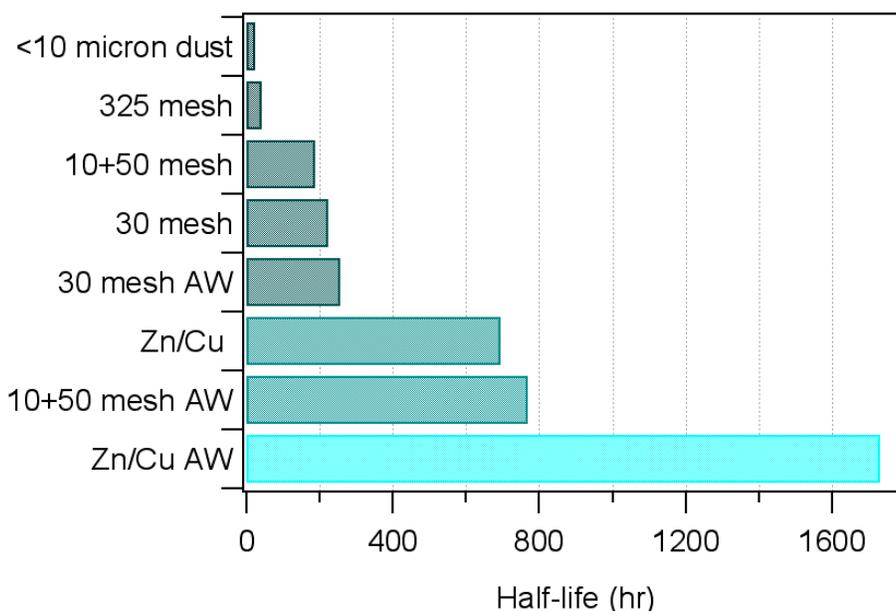
Figure 10. Disappearance rates (plotted as half-lives) for eight types zinc power in DI Water. These data are not corrected for differences in surface area. "Zn/Cu" is bimetallic Cu on Zn. "AW" stands for acid washed.

Much of our experimental work during PY3 was focused on verifying the promising initial results that we obtained with ZVZ. To this end, a variety of experiments were performed in batch reactors. The first large set of experiments was done with a variety of reagent-grade samples of ZVZ, and the results are summarized in Figure 11. Note that these data are uncorrected for differences in specific surface area, but they do represent a valid comparison on the mass normalized basis because all the experiments were done with the same mass of ZVZ to solution volume ratio. Three general conclusions are apparent from Figure 11: (*i*) the kinetics of TCP disappearance are pseudo first-order, (*ii*) some of the treatments gave quite rapid disappearance of ZVZ

with $t_{1/2}$ ca. 1 day, and (*iii*) the site water sample gave slower TCP degradation rates than the DI water. Further investigation and interpretation of the latter result is given below.
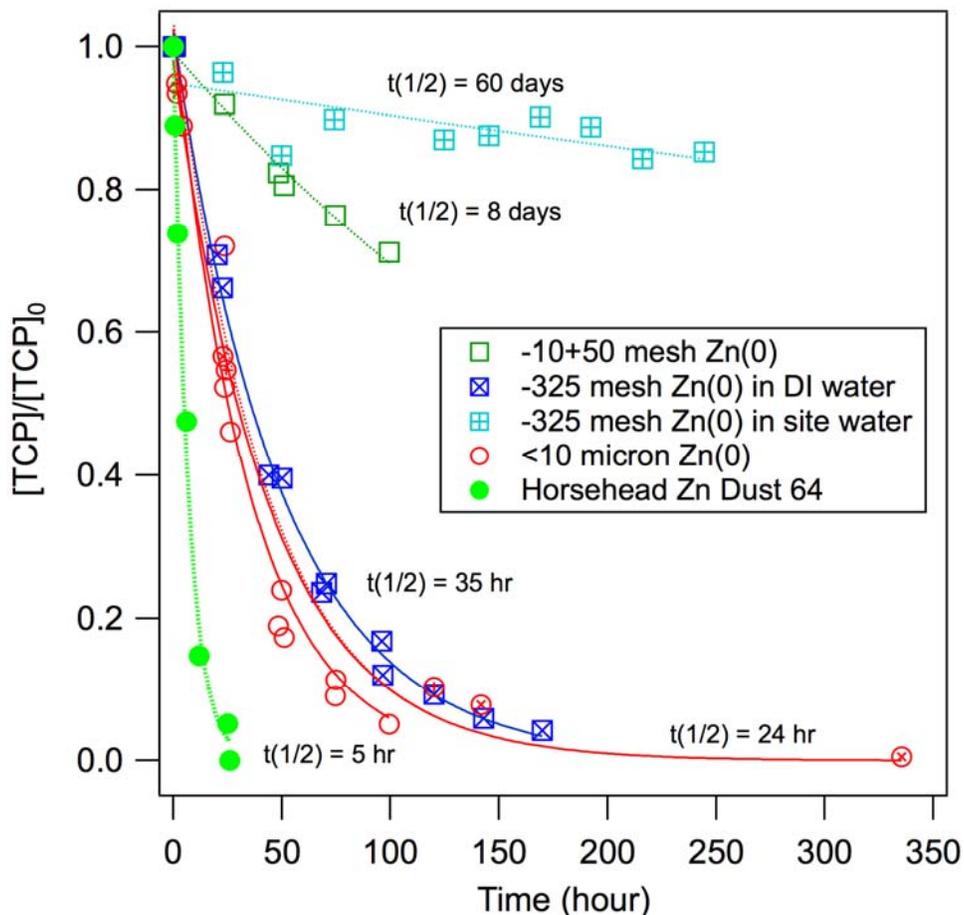
Figure 11. Kinetics of TCP disappearance with several types of reagent grade zero-valent zinc (ZVZ) in batch reactors made with deionized water or with a groundwater from an agricultural site in California. Replicates for the treatments shown in red and blue were deemed to be identical, so they were pooled and fit as one.

As part of one of our other projects on contaminant degradation with zero-valent metals, we have developed a suite of electrochemical methods for characterization of the zero-valent metals used in remediation. The methods are flexible and robust and are easily applied to ZVZ. So far, with ZVZ, we have performed several sets of electrochemical experiments using conditions similar to the batch experiments shown in Figure 11. The two electrochemical methods are chronopotentiometry (CP) and linear sweep voltammograms (LSV), and one set of these results obtained with these methods is shown in Figure 12, Parts A and B, respectively.
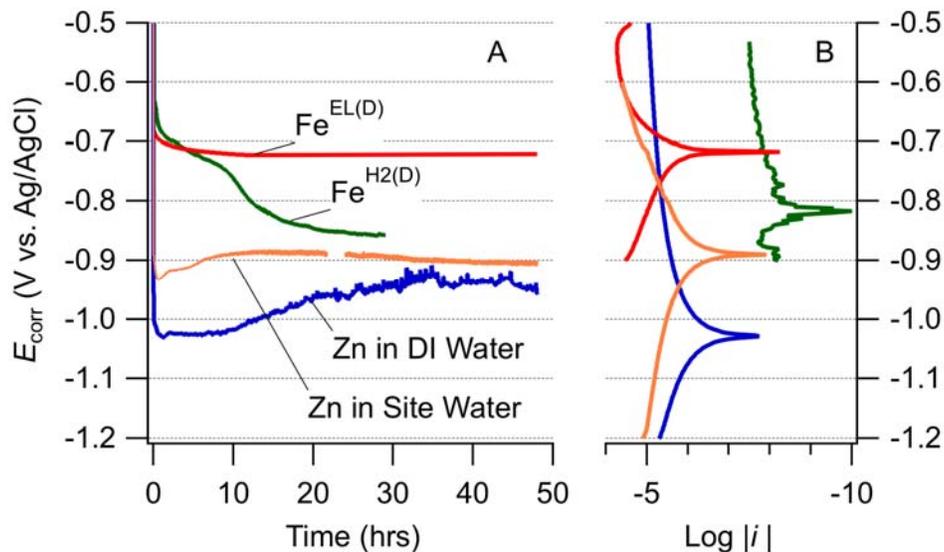
Figure 12. (**A**) Open circuit chronopotentiograms, CPs, and (**B**) linear sweep voltammograms, LSVs, obtained with stationary powder disk electrodes (PDEs) of Fisher electrolytic Fe^0 ($Fe^{EL(D)}$), Toda RNIP nano-sized Fe^0 ($Fe^{H2(D)}$), and Aldrich 30 mesh Zn^0 powder (Zn). The data for Fe^0 are the same as data that we published and discussed in (*12*). All of these results were obtained in deoxygenated deionized water. Based on independent measurements (not shown), the pH in these systems should rise to about 10 over 6 hr, and then stabilize.

The layout of Figure 12 follows a format that we used extensively in a previous publication (*17*). Both parts are shown with potential on the ordinate, thereby helping to convey convergence of the CP data to characteristic potential regions (active, passive, etc.) defined by the LSV data. The LSVs were obtained by ramping (at 0.1 mV s^{-1}) the applied potential anodically, where the cathodic current is mainly due to reduction of H_2O to H_2; to E_{corr} (the singularity), where anodic and cathodic partial currents are equal; through the active region, where dissolution of the metal dominates; and finally into the pre-passive and passive region, where current decreases sharply due to formation of passivating oxides. The noise in the CP for Zn is due to formation of H_2 bubbles on the electrode

That data in Figure 12 indicate that the passivating oxide film on Zn^0 breaks down immediately upon immersion into water and then the surface partially repassivates over the remaining time period of our experiments. Comparing these results with data for two representative types of Fe^0 (also included in Figure 12 for comparison) shows: (*i*) that depassivation of Fe^0 may exhibit a characteristic delay that is not seen with Zn^0, (*ii*) that the limiting potentials for Fe^0 are significantly less negative than Zn^0, and (*iii*) repassivation of Fe^0 was not evident in the time period where it occurs with Zn^0. The practical implications of these conclusions are not yet completely clear, but they suggest

that the corrosion of Zn^0 and Fe^0 have complementary characteristics that might be used to advantage in remediation applications.

In Figure 11, we also include a sample of our most recent results using industrial grade ZVZ powder. The data are for Zinc "Dust 64" from Horsehead Corporation, which sells zinc in various forms recycled from various sources (somewhat like the companies that sell scrap granular iron metal for PRB applications). The ZVZ from Horsehead appears to be at least as reactive as the laboratory-grade materials (recall that these data are not surface area normalized yet). We have done more extensive investigation with several forms of ZVZ, which we have obtained from the Horsehead Company for a pilot study that is part of a separately funded project.

A more precise view of the relative reactivity of ZVZ is provided by Figure 13. This k_{SA} vs. k_M plot shows that the rate constants from these experiments are 1.0 (for k_M)
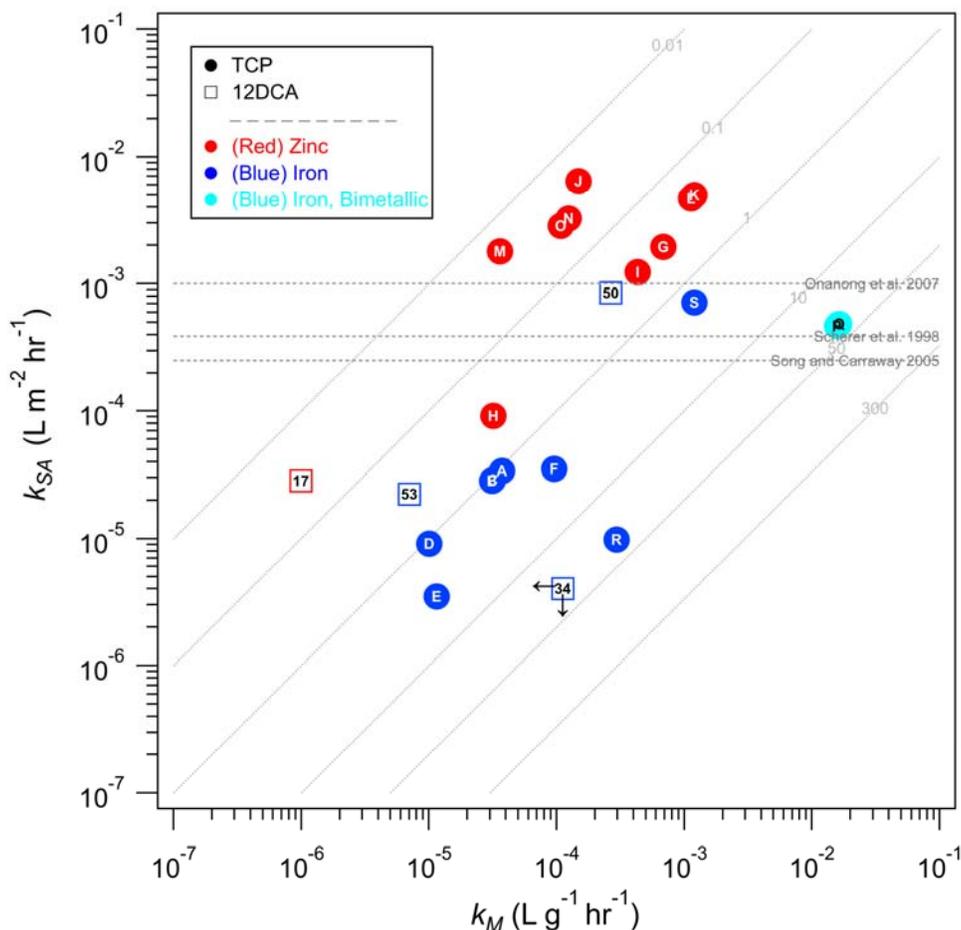
Figure 13. Mass-normalized rate constants (k_M) and the corresponding surface-area normalized rate constants (k_{SA}) for reduction of TCP and related chlorinated aliphatics by Zn^0 and Fe^0. Diagonal lines are contours for representative values of ρ_a (m^2 g^{-1}). Horizontal lines represent k_{SA}'s for TCP and Fe^0 estimated from QSARs previously published in the noted sources.

to 2.5 (for k_{SA}) orders of magnitude higher for Zn^0 than Fe^0. Most the data for TCP and Zn^0 were obtained under the same experimental conditions, except for the type and pretreatment of the Zn^0. The effect of Zn^0 type is typical of materials with similar composition (and therefore surface reactivity) but different morphologies (and therefore specific surface areas): the k_M values cluster in two groups—at 10^{-3} and 10^{-4} L g^{-1} hr^{-1} for fine grain and course gain Zn^0, respectively—but all the groups become one cluster (k_{SA} $\approx 5 \times 10^{-3}$ L m^{-2} hr^{-1}) after normalization to the specific surface area for each Zn^0 type.

While the focus of Figure 13 is on relative rates of TCP reduction, we can use the format to provide a broader perspective by including representative data from previous studies on reduction of other contaminants. Adding selected kinetic data for chlorinated methane, ethanes, and ethenes gives Figure 14. The figure contains all the relevant kinetic data for dechlorination by Zn^0, and reveals a very wide range of reactivity with Zn^0 (6 orders of magnitude in k_{SA}), with TCP falling roughly in the middle. The pattern of

Figure 14. Extension of the k_{SA} vs. k_M plot analysis shown in Figure 13, including data for a wide range of other chlorinated solvents for comparison.

reactivity is generally consistent with expected trends (e.g., faster rates with higher degree of chlorination, chlorinated alkanes faster than alkenes), but some of the relationships suggest combinations of factors (e.g., TCP reacts at about the same rate as 1,1-DCA and much faster than 1,2-DCA) that merit further consideration and are discussed further below. In addition to the data for Zn^0, Figure 14 includes all the relevant kinetic data for reaction of TCP with Fe^0, and a few additional data for related reductants (e.g., Fe^0/Pd) and analogous oxidants (e.g., 1,2-DCA).

We have begun working on trying to extend the analysis in Figure 14 into a full correlation analysis that might eventually lead to quantitative structure-activity relationships (QSARs) for reduction of halogenated aliphatic compounds by zinc and other ZVMs. This requires calculation of descriptor variables for the target compounds, which we have done (not shown), but it would help to have some additional calibration data beyond what is shown in Figure 14. A few such measurements were made. An example is shown in Figure 15, which shows the disappearance kinetics of 1,2-dichloropropane (DCP) under conditions identical to those used in some of our batch experiments with TCP.
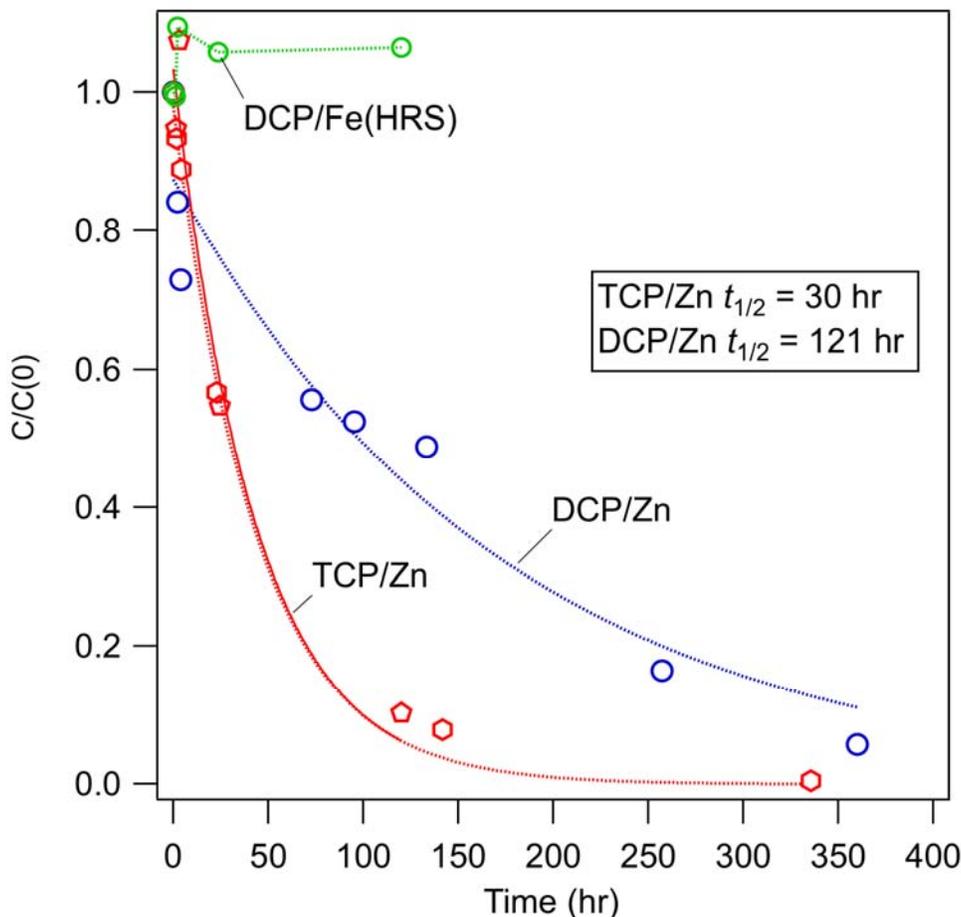
Figure 15. Disappearance kinetics for DCP, with TCP for comparison, in batch reactors containing various ZVZ. These data are for the commercial-grade ZVZ obtained from the Horsehead Corp.

Tasks 3.4 to 3.6: *Fe₃O₄ and Fe₂O₃ w/ or w/o Fe²⁺, or FeS.*

Based on the results of the preceding tasks, we did not expect the milder Fe(II)-based reductants to produce measurable dechlorination of TCP, but we did done some exploratory experiments to verify this. Nano-sized goethite (Fe_2O_3) and magnetite (Fe_3O_4) were used in reaction vials with and without 1 mM FeCl₂ otherwise exactly according to the method described for homogenous systems. As shown in Figure 17, none of the Fe^{II} systems showed significant TCP degradation within the time frame of our experiment (30 days). These experiments were not pursued further. FeS (Task 3.6) was not tested. To balance the figures, we have included results from Pd/Fe in Figure 17, although they were discussed above under the corresponding task (3.3).
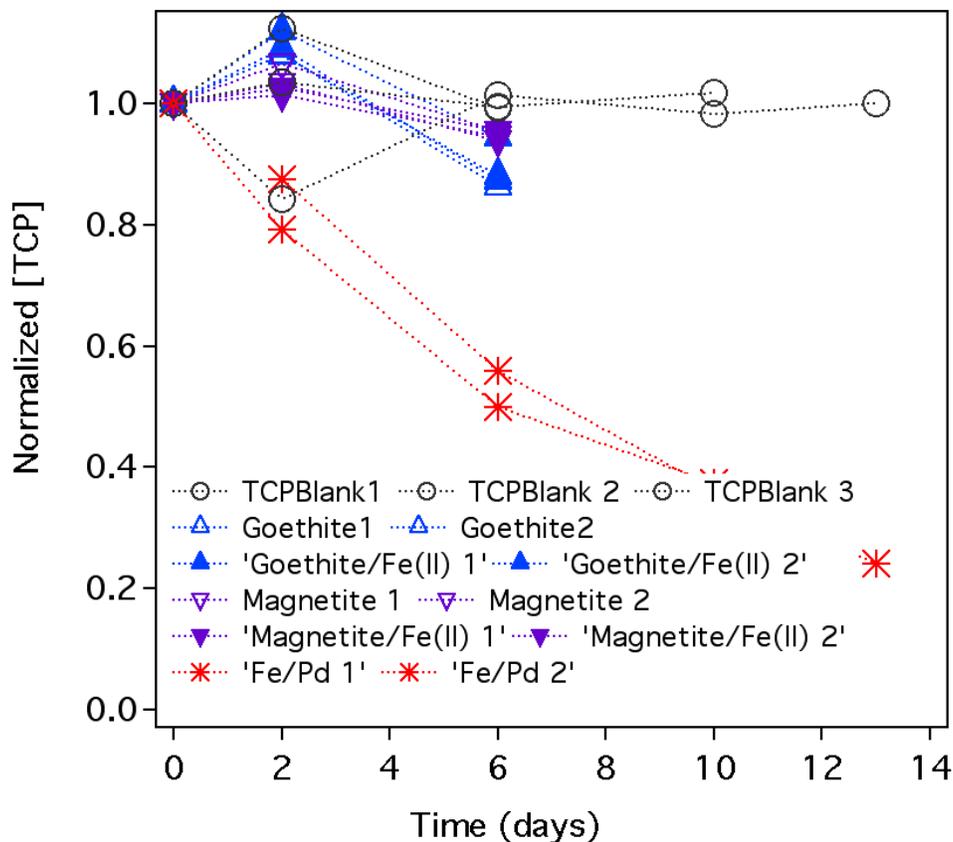
Figure 16. Disappearance kinetics for TCP in batch reactors containing various iron-based reductants. The experiments with goethite and magnetite show no loss of TCP and there is no loss due to adsorption

Homogeneous Oxidation Reactions[4]

Task 4.1: Peroxide

For this task, we have used procedures similar to those that we have developed for our previous SERDP project on in situ chemical oxidation (CU-1289). The reactor we use consists of a 100 ml airtight glass syringe (Hamilton, Reno, NV) attached to a syringe pump (KD Scientific, New Hope, PA). A 3-way Luer-lock valve (Kontes Glass Company, Vineland, NJ) is used for addition of hydrogen peroxide and for removal of samples. The solution is stirred in the reactor with a micro stir bar and a 'Spinette' Electric Cell Stirrer (Starna Cells Inc., Atascadero, CA Model SCS 1.11). The procedure is: (i) mix contaminant plus $FeSO_4$ with freshly prepared stock solutions, (ii) adjust pH to

---

[4] The results on TCP degradation with ISCO type oxidants shown here has not been published elsewhere.

3.0 with H_2SO_4, (iii) add >50 ml reaction mix to 100 ml air tight syringe, (iv) adjust volume to 47.5 ml, (v) inject 0.5 ml sample for t = 0, (vi) add 3.0 ml H_2O_2 stock to small syringe, (vii) add H_2O_2 to 100 ml air tight syringe to start reaction, (viii) mix for 1 minute, (ix) take samples at predetermined times. Samples are added to 5 ml hexane and shaken for 15 minutes. 1 ml hexane extract is used in GC analysis as described in Task 1.1.

We performed two series of experiments with TCP under classical Fenton conditions. The results, shown in Figure 17, show that TCP is degraded at a substantial rate. After a brief initial drop, the disappearance of TCP appears to be first-order with a half-life of 5-10 hr. However, the overall kinetics are not simply pseudo first order and suggest the more complex, bimodal behavior that is often observed with Fenton systems. Although it is easy to rationalize the bimodal kinetics—due to a shift from Fe(II) to Fe(III) catalyzed decomposition of H_2O_2—it is more difficult to model such kinetics quantitatively. So far, we have not been successful at modeling this particular data set. A previous study found that products of Fenton degradation of TCP include 1,3-dichloroprop-anone, chloroacetic and formic acids (*18*).
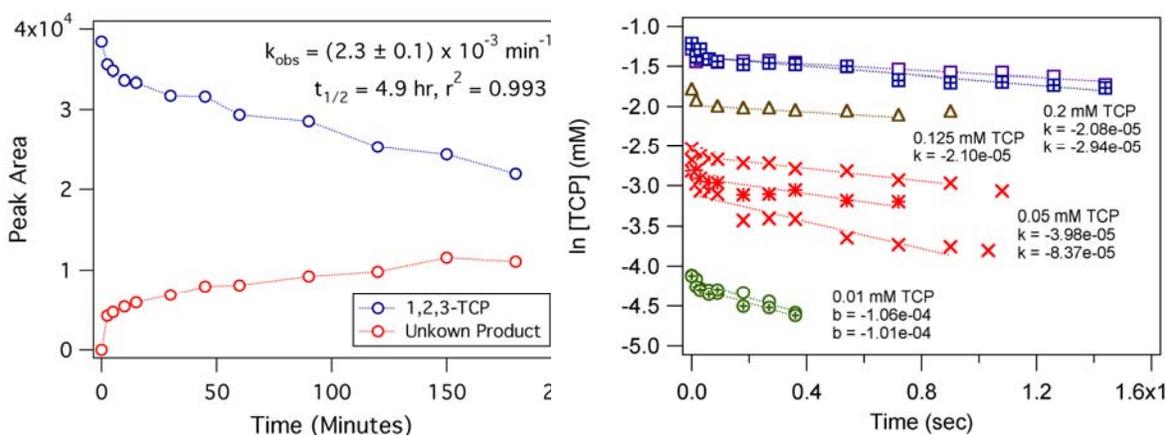
Figure 17. Results from batch experiments under classic Fenton conditions. (1,2,3-TCP = 0.05 mM, H_2O_2 = 300 mM, $FeCl_2$ = 25 mM, pH = 2.9, T = 25°C).

Task 4.2: Ozone

We did not perform any experiments with ozone. Based on our other results, however, we expect that TCP will be degraded in so far as the conditions of ozonation favor formation of hydroxyl radical (*19*). Direct reaction of ozone with TCP is likely to be slow, much in the same way that oxidation of TCP with permanganate is slow (See Task 4.4).

Task 4.3: Persulfate

A series of preliminary experiments showed, as in Figure 18, that TCP is rapidly oxidized by persulfate activated by heat. We varied the initial dissolved oxygen concentration to see if dissolve oxygen might be activated as a side effect of sulfate radical chemistry, thereby providing additional pathways for TCP degradation and faster degradation rates.
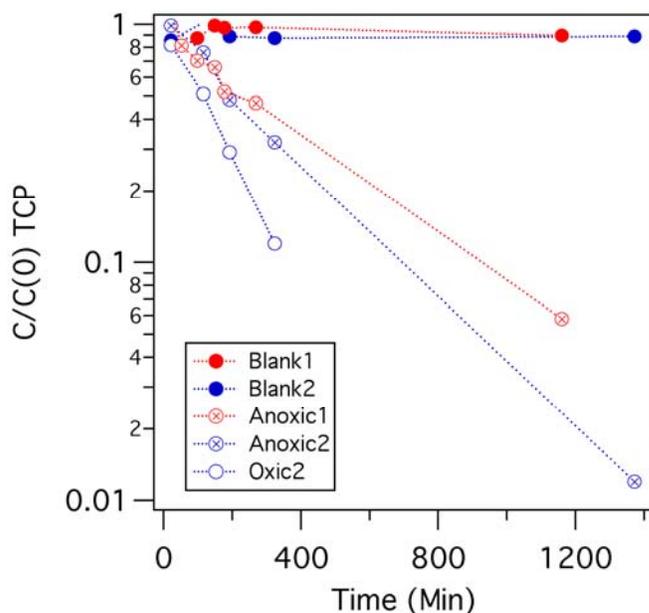
Figure 18. Pseudo first-order disappearance kinetics of TCP in unbuffered, heat activated, persulfate. Fitting these data gives k_{obs} = 0.15-0.19 hr^{-1} and $t_{1/2}$ = 4 hr for anoxic conditions, and k_{obs} = 0.39 hr^{-1} and $t_{1/2}$ = 1.8 hr for oxic conditions.

Concurrent with the experiments shown in Figure 18, we measured chloride and CO_2 concentrations to assess the degree to which TCP degradation resulted from dechlorination and mineralization, respectively. These results are summarized in Table 7.

Table 7. Summary of products from TCP oxidation with activated persulfate.

Treatment	Time	Final Cl$^-$	Time	Final CO_2
Oxic	6.1 hr	0.38 mM (74%)	--	--
	23.4 hr	0.48 mM (84%)	--	--
Anoxic	6.5 hr	0.24 mM (71%)	3 hr	0.076 mM (36%)
	23.5 hr	0.40 mM (86%)	26 hr	0.42 mM (88%)

The encouraging results shown in Figure 18 led us to perform follow-up experiments. One significant result is shown in Figure 19; which employs the competition kinetic method we have used recently to measure second-order rate constants for reaction of contaminants with sulfate radical. In this case, the competition is between

TCP and the probe p-nitroso dimethylaniline (RNO). Fitting of these data gives a second-order rate constant for TCP reaction with sulfate radical, $k'' = 2.7 \times 10^6 \, M^{-1} \, s^{-1}$
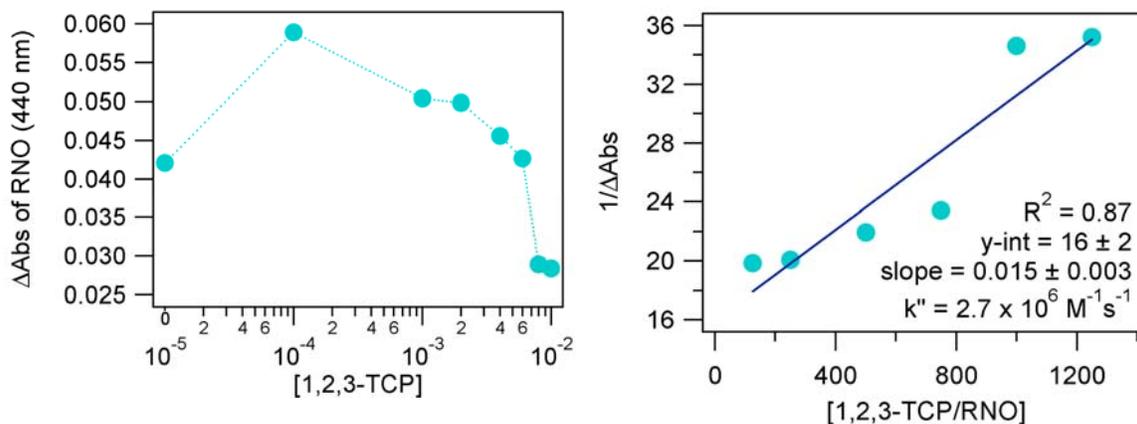
Figure 19. Preliminary competition kinetics for TCP degradation by activated persulfate. Light activation, pH = 9.

Now that we have an estimate of k" for reaction of TCP with sulfate radical, we can ask how its reactivity with sulfate radical compares to that of other organic contaminants. Fortunately, we already have the rest of the kinetics data necessary for such a comparison, in large part due to our work on the "IscoKin" database.[5] Superimposing our estimate of k" for TCP on a plot of all the available data for environmentally relevant aliphatics gives Figure 20.

---

[5] Unrestricted access is available from http://cgr.ebs.ogi.edu/iscokin/.
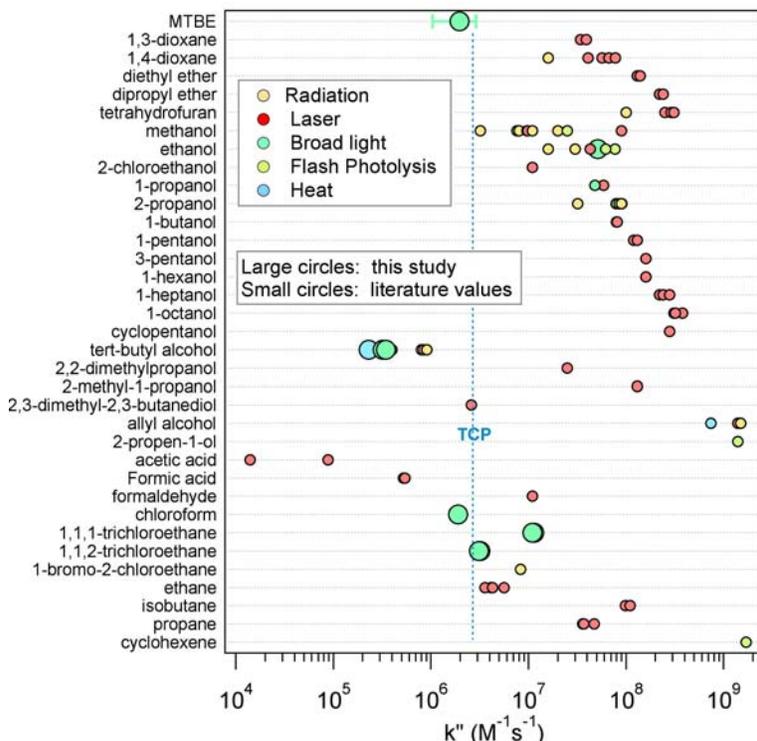
Figure 20. Comparison of all available second-order rate constants for reaction of sulfate radicals with environmentally relevant aliphatic organics. The large circles are values that we measured for another project. The color coding shows that the method of persulfate activation does not have any necessary effect on k".

From Figure 20, we see that our estimate of k" for TCP is in line with that of other closely related compounds (e.g., chlorinated ethanes), but that these are relatively unreactive compared to most aliphatics. While this is true, most of the values of k" are large enough to give rapid degradation when formation of sulfate radical is efficient.

Task 4.4: Permanganate

Preliminary experiments with permanganate (performed while preparing the proposal for this project) were not revisited, but the data are shown in Figure 21. First, the disappearance of 1,2,3-TCP is considerably faster than comparable compounds for which we have data, such as 1,2-dichloroethane (1,2-DCA). Second, the kinetics are not simply pseudo first-order, but suggest a fast first-order process followed by a slower one (bimodal fit). This could be due to impurities in the 1,2,3-TCP standard that we used (new and nominally 99% pure from Sigma-Aldrich). Mass spectrometry on this standard identified several impurities that might be responsible for the fast initial reaction shown in Figure 21, including mono-, di-, and tri-chloropropenes.
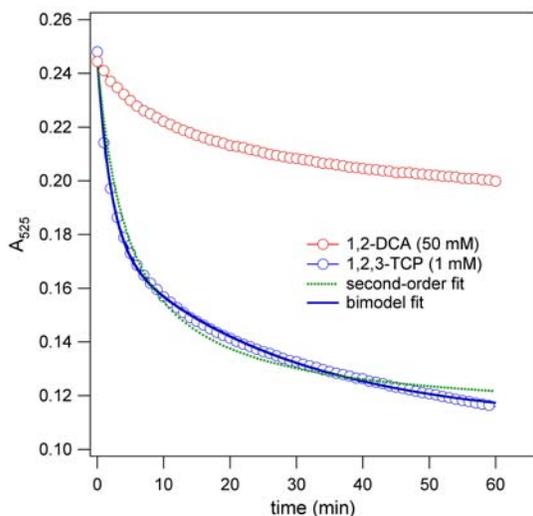
Figure 21. Disappearance of TCP and DCA in permanganate. ($KMnO_4$ = 0.1 mM, pH = 7.0, T = 25°C)

Optimize Selection of ZVZ

Task A1. Screening Industrial-Grade ZVZ Materials.

Three commercially available materials provided by Horsehead Corporation (Monaca, PA) were selected for screening; the material properties are summarized in Table 8. TCP disappearance kinetics using these materials were measured in batch reactor experiments containing TCP spiked deionized (DI) water and deoxygenated DI water (DO/DI) (Figure 22)[6]. Zn64 degraded TCP at the fastest rate, and the rate did not appear to be effected by the presence or absence of oxygen. Degradation of TCP by Zn1210 was slower (by about one order of magnitude), but again did not appear to be effected by the presence of oxygen. Zn1239 gave TCP degradation kinetics similar to Zn1210 in DO/DI water (despite its higher surface area), but much slower rates in the presence of oxygen (Figure 22).

The observed rates obtained in these batch experiments were normalized to mass to obtain a mass-normalized rate constant (k_M) and compared to previously measured (4) rates obtained with reagent grade ZVZ. These results are shown in Figure 23. It can be seen that, for the most part, the k_M values obtained using industrial-grade ZVZ fall within the range of values obtained with reagent grade material. The exception to this is Zn1239 in the presence of oxygen, which showed much slower kinetics.

---

[6] These results have been published in the Proceedings of the 7th International Conference on Remediation Chlorinated and Recalcitrant Compounds (20).

Table 8. Industrial-Grade ZVZ Properties.

Material	Designation	Mesh[1]	Specific Surface Area (m^2/g) [2]	Bulk Density (g/mL)
Zinc Dust 64	Zn64	through 325	0.620	2.60
Zinc Powder 1210	Zn1210	20-60	0.016	2.34
Zinc Powder 1239	Zn1239	200-325	0.160	3.27

[1] Provided by manufacturer. [2] Measured by BET gas adsorption.
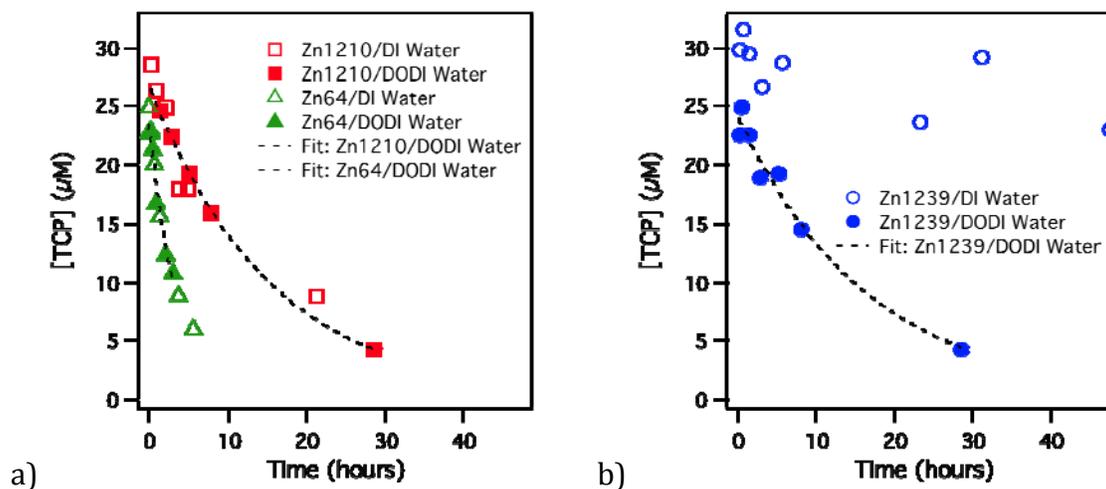
Figure 22. (**A**) Degradation of TCP by Zn64 and Zn1210 in DO/DI and DI water. (**B**) Degradation of TCP by Zn1239 in DO/DI and DI water. In both figures, solid symbols represent DO/DI data, with fit curves shown. Hollow symbols represent data from unsparged DI water batches. All batches contained an equal mass dose of ZVZ (250 g/L).
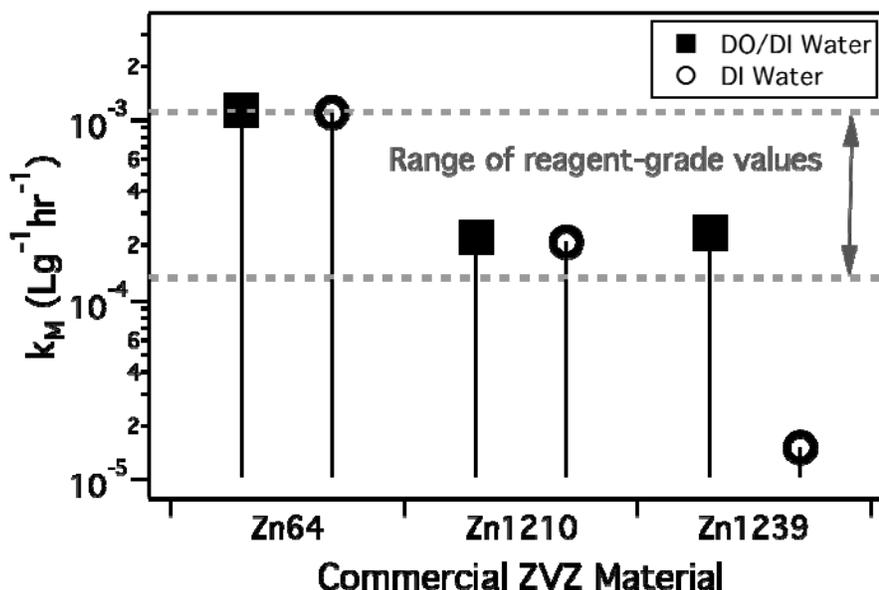
Figure 23. Mass normalized rate constants (k_M) for TCP degradation by three commercial ZVZ materials in DI water with and without dissolved oxygen. Gray dashed lines represent the range of k_M values reported previously using reagent-grade ZVZ (*4*).

Another method of comparing the rates obtained with industrial-grade material to the rates obtained with reagent-grade material is to display the data on a k_{SA} vs. k_M plot (Figure 24). This plot contains information about the mass-normalized rates, as well as surface-area-normalized rates (k_{SA}). Because of this, it contains more information about the fundamental reactivity of the materials than is shown in a plot that exclusively compares k_M values. Figure 24 shows that, while Zn64 is more reactive towards TCP on a mass-normalized basis, Zn1210 is more reactive on a surface-area-normalized basis. It is unclear which normalization method is a better indicator of general field performance, as this will likely be a function of various treatment method drivers (e.g., although Zn1210 is fundamentally more reactive on a surface-area normalized basis, the small size of Zn64 allows for a greater mass of material to fit in volume limited systems resulting in faster kinetics produced by Zn64 than Zn1210 in systems with identical volumes such as columns).
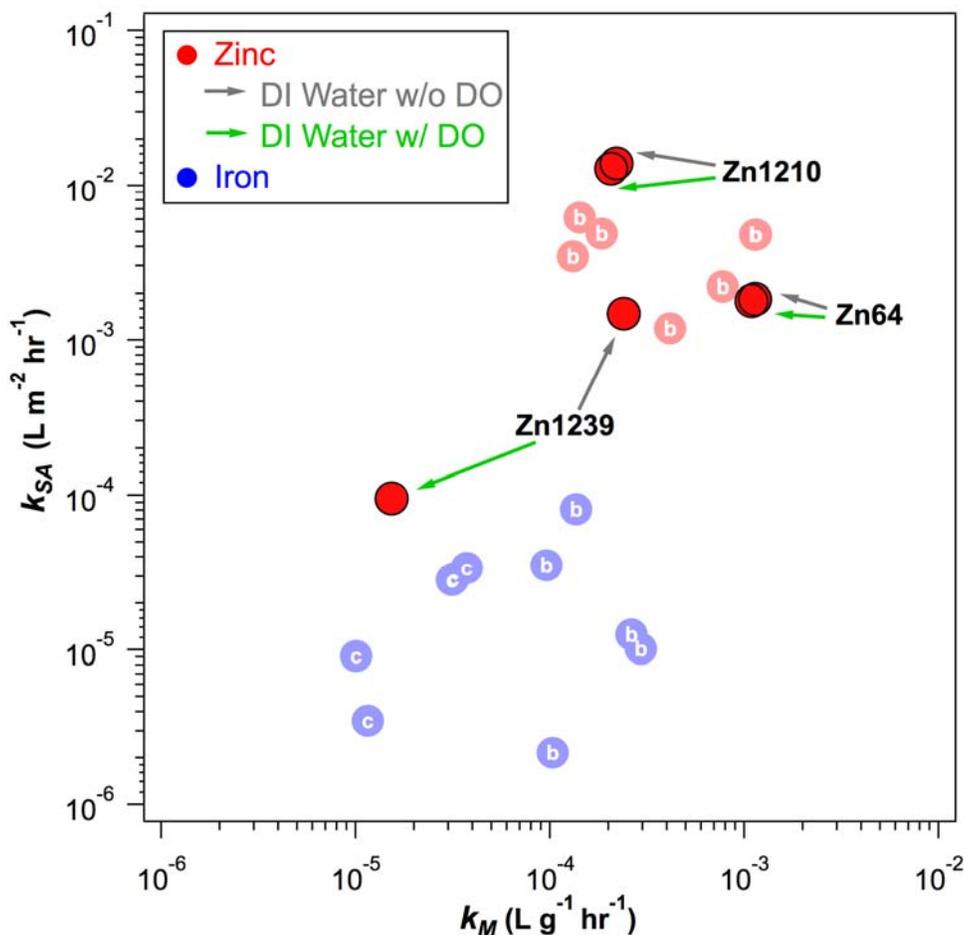
Figure 24. Comparison of TCP degradation kinetics by industrial-grade ZVZ materials to values gathered with reagent-grade ZVZ and various zero-valent iron (ZVI) materials as reported in (*4*). Kinetics were measured in DI water with and without dissolved oxygen. Kinetics in the presence of reagent- and industrial-grade ZVI (as reported in (*4*)) are shown for comparison.

Task A2. Nano ZVZ

Synthesis of nZVZ through borohydride reduction of ZnCl was attempted. While the material appeared to degrade TCP, the results could not be compared to those using granular zinc, as the amount of nanozinc synthesized (and therefore the zinc load) could not be measured. Excessive hydrogen production was a major problem.

Commercially available nZVZ was purchased from Strem Chemicals (Newburyport, MA). This material showed promising reactivity with TCP, especially on a mass-normalized basis. Figure 25 shows where Strem nZVZ falls on the k_{SA} vs. k_M plot relative to the industrial-grade ZVZ and other ZVZ and ZVI materials. Strem nZVZ showed similar k_{SA} values to the other ZVZ materials, but k_M values 1-2 orders of magnitude faster.
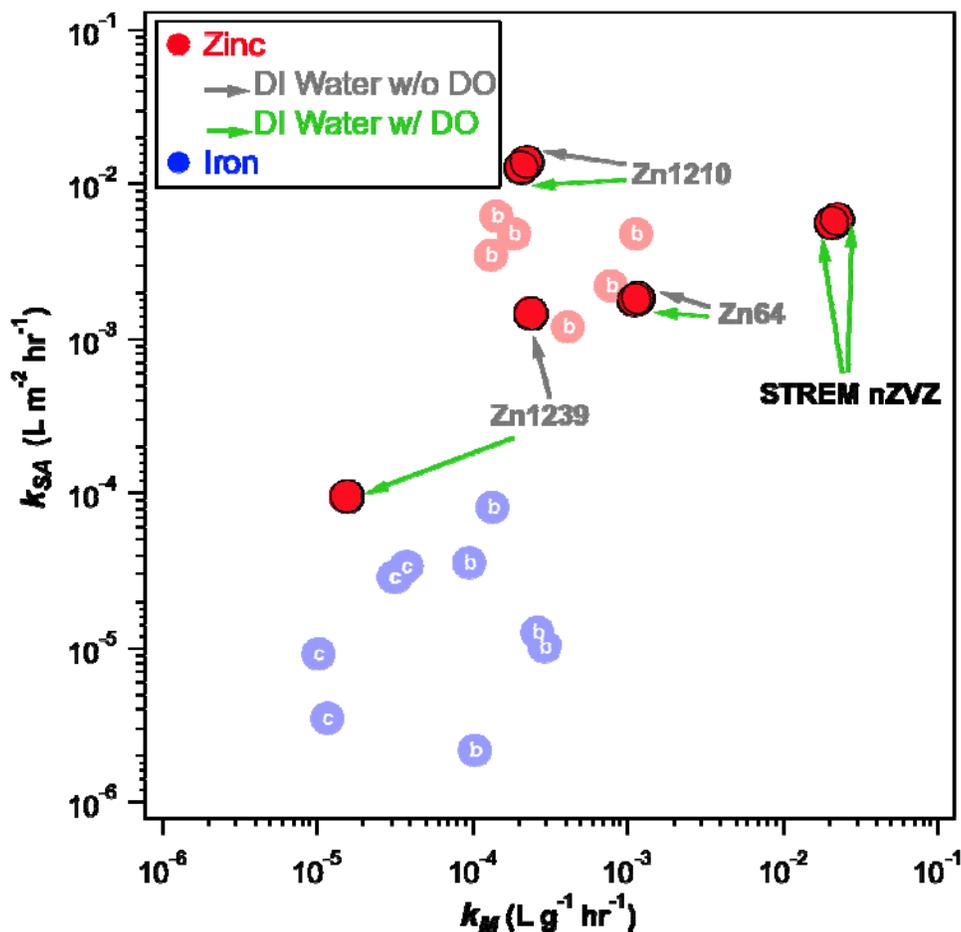
Figure 25. Comparison of nZVZ rates to rates gathered with industrial-grade ZVZ and to previously reported (*4*) ZVZ and ZVI rates.

Task A3. Bimetallic (Nano)particles

Degradation of TCP with Z-Loy (OnMaterials, Escondido, CA), a nanoparticulate Al/Fe/Zn material, was attempted. The material could not be sufficiently cleaned of its propylene glycol "packaging", making mass measurements difficult. Hydrogen gas was produced at such a rate that continued analysis was unsafe using current methods.

Attempts were made to increase ZVZ reactivity by palladizing Zn64 to produce a Zn^0/Pd^0 material. The TCP degradation kinetics using this material are shown in Figure 26. As the typical palladization process includes acid washing, acid washed ZVZ was also tested as a control. Contrary to the ZVI results, it was seen that palladization decreased ZVZ reactivity towards TCP.
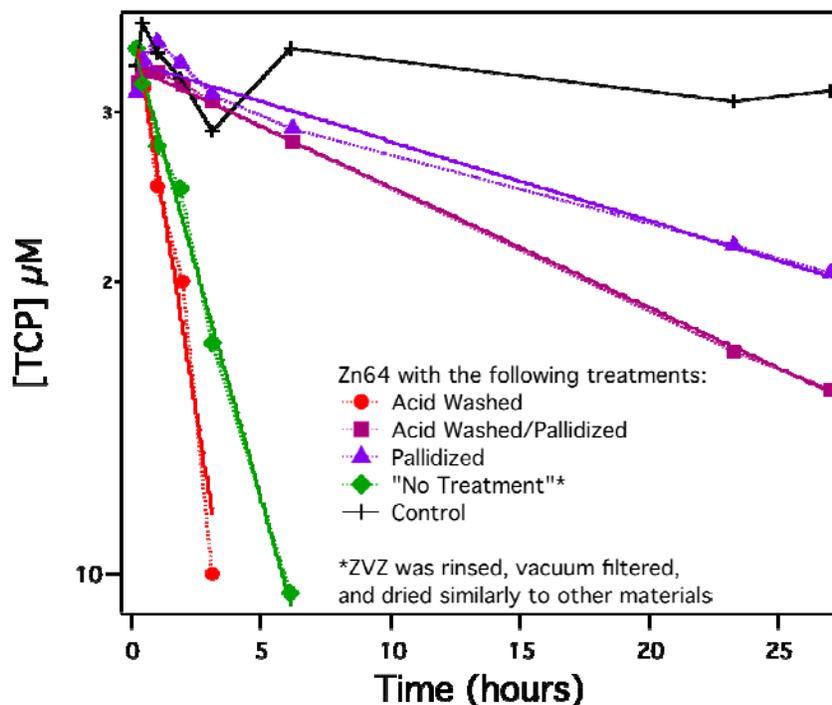
Figure 26. Disappearance of TCP in the presence of ZVZ (Zn64) with various treatments including palladization. Palladization was seen to slow TCP degradation kinetics.

Task A4. Inter-Metallic Effects (Fe^0 and Zn^0 Alloys).

Inter-metallic effects were not investigated.

Optimization of the ZVZ Process for TCP

Task B1. Effect of Water Chemistry in Batch Experiments.

Effect of Groundwater and Groundwater Constituents

The kinetics of TCP degradation by Zn64 were measured in three groundwaters from different sites in Washington and California. Results are shown in Figure 27. In all cases, TCP degradation occurred at much slower rates in site water than in DI water. In an attempt to identify the inhibitory effect of site water, TCP degradation kinetics were measured in a variety of artificial groundwater (AGW) solutions containing individual groundwater constituents, at or above the concentration reported for one of the groundwater sites (raw data shown in Figure 28, k_M values shown in Figure 29). Phosphate and silicate were the only constituents evaluated that appeared to slow the degradation of TCP. Silicate displayed inhibition at the reported site water concentration;

phosphate only displayed inhibition at a concentration higher than the reported value (no inhibition was seen in an AGW solution containing the reported site water concentration).
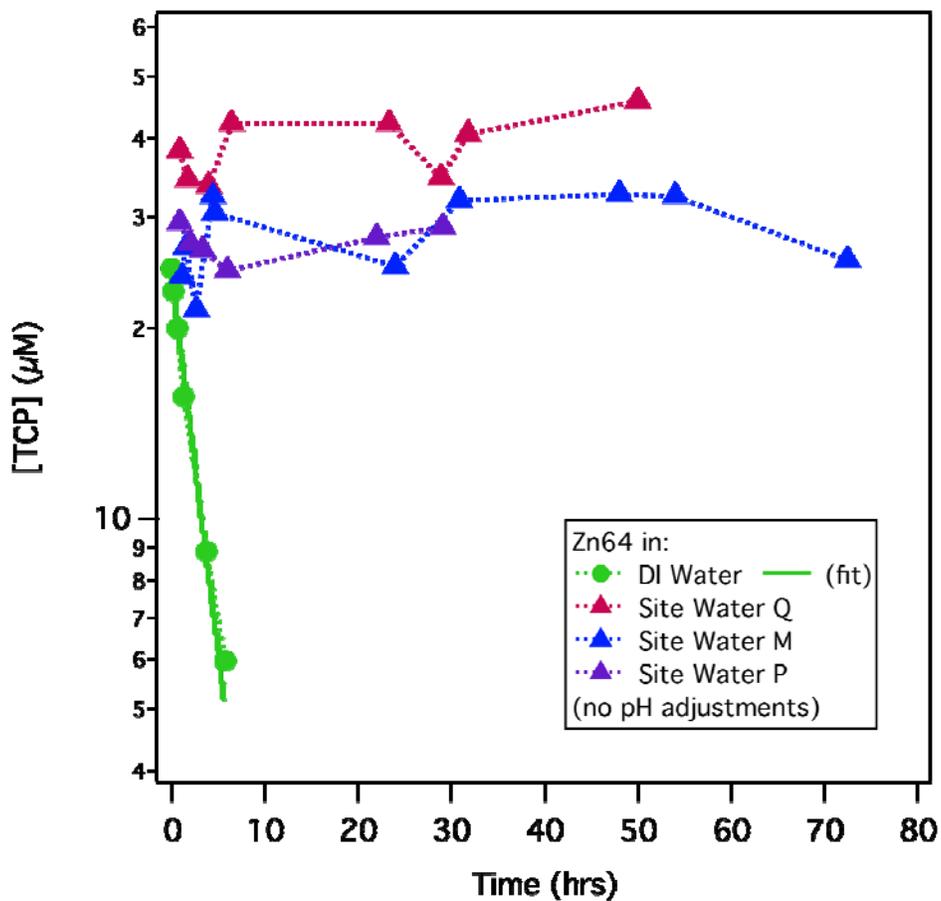
Figure 27. Degradation of TCP by Zn64 in DI water and various site groundwaters.
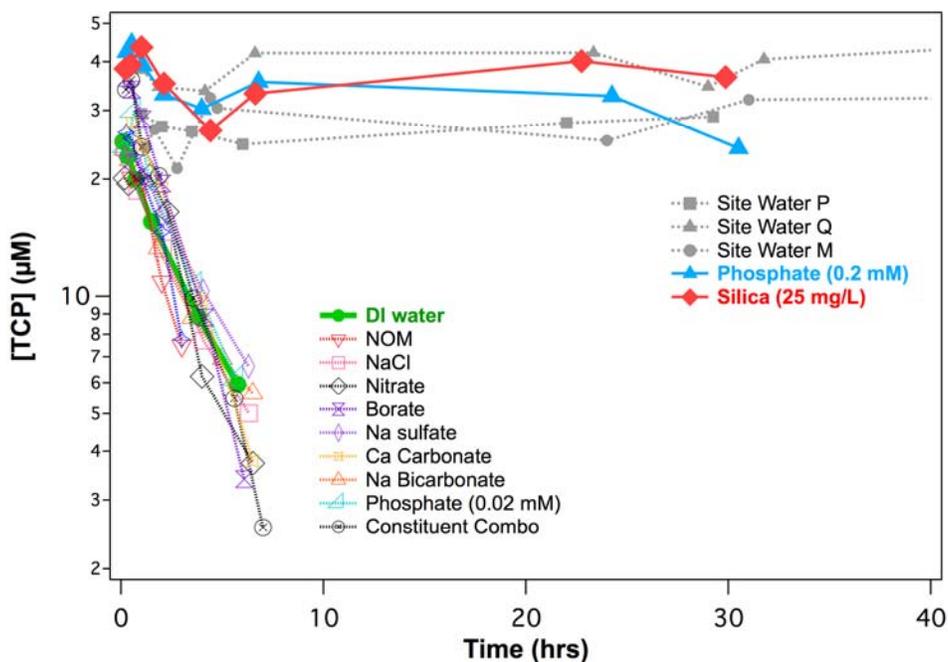
Figure 28. Degradation of TCP by Zn64 in DI water, site water, and various artificial groundwaters prepared at or above the concentration reported for Site Water P.

Effect of Silica Sand

The inhibitory effect observed with silicate and the prevalent use of silica sand in current zero-valent metal treatment systems led us to study the effect of adding silica sand to batch-reactor experiments. Zn64 was used for these experiments as the small mesh of Zn64 will likely necessitate the material be mixed with sand in treatments systems to avoid excessive backpressure and clogging. Batch reactors containing equal mass loads of Zn64 but differing amounts of sand were run. As seen in Figure 30, sand was seen to inhibit TCP degradation such that, the greater the ratio of sand to zinc, the slower the TCP degradation rate. The effect of pH on batch reactors containing Zn64 and sand was also assessed. It was seen that TCP was degraded more quickly at pH 6.9 than it was at 9.3 or 11.6 (Figure 31). This result agrees with the trends seen in both site water and silicate AGW.
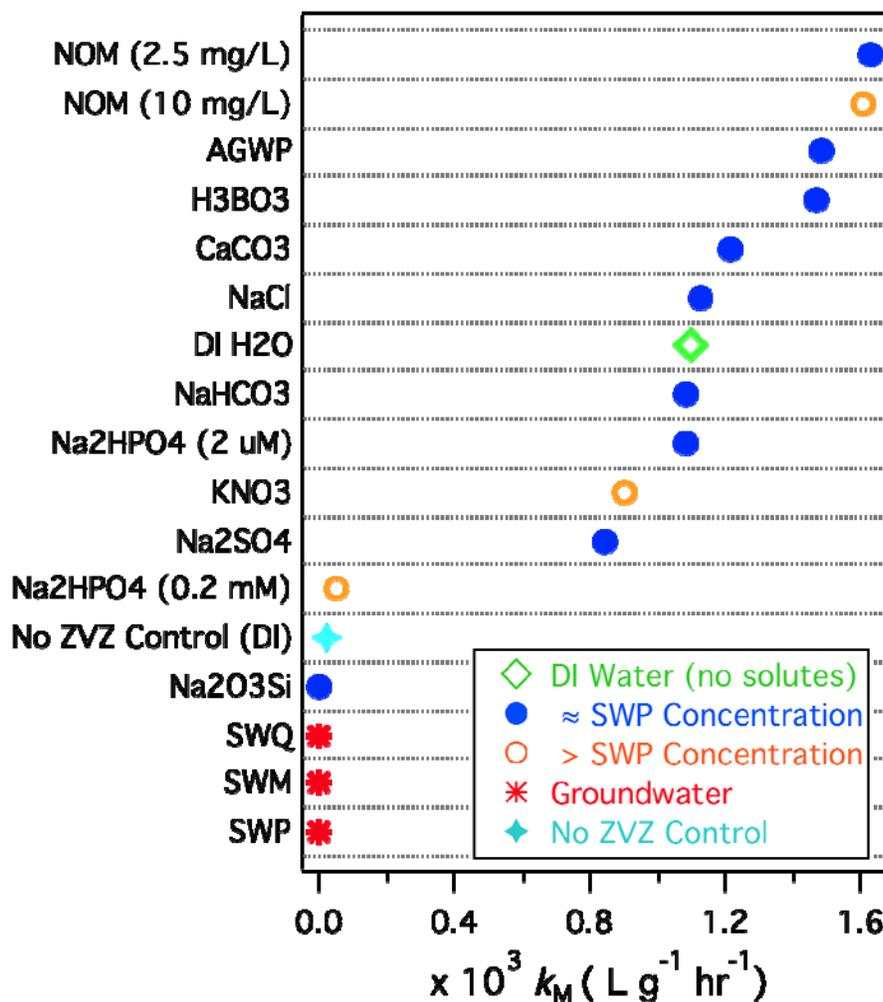
Figure 29. k_M values obtained from observed values shown in Figure 28 for TCP degradation by Zn64 in DI water, site groundwaters P, Q, and M, and various artificial groundwaters prepared at or above the concentration reported for Site Water P (SWP).

The question arouse as to whether or not the inhibition seen in the presence of sand was a result of dissolved silicate or material contaminating the sand surface that—in effect—transformed the DI water in the batch reactor to site water. To evaluate this, an additional batch experiment was run with sand that had been rinsed a number of times with DI water (Figure 32). This batch experiment displayed faster TCP degradation kinetics than the reactor containing sand that had not been cleaned, however, the kinetics were still not as fast as those in DI water without sand.

Another question that arose was whether or not the inhibitory effects of sand and groundwater were additive. We tested this by comparing the kinetics of TCP reduction in two batch reactors, both containing an equal mass ratio of Zn64 and sand, but either in DI water or groundwater. The results are shown in Figure 33. We observed that, at low pH

(~6.9), the TCP degradation kinetics using a 1:2 mixture of Zn64 to sand appeared unaffected by whether DI water or site water was used in the batch reactor. This suggests that, at this pH, inhibition by sand and site water are not additive.
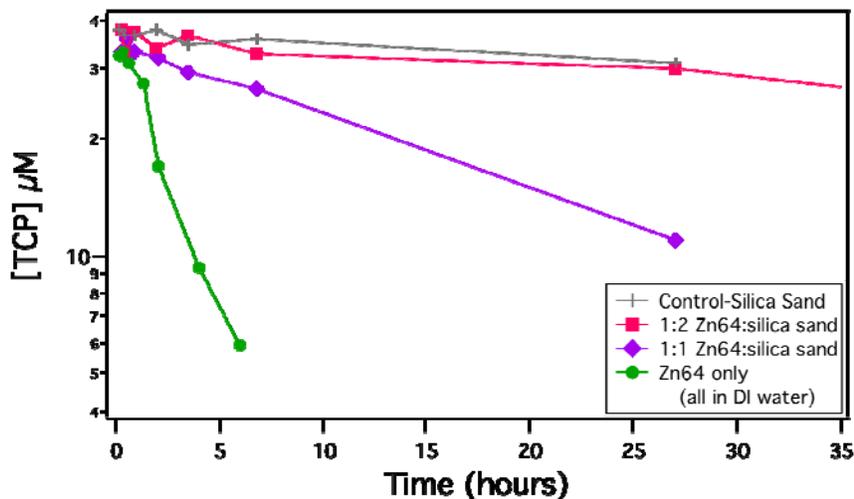
Figure 30. TCP degradation in batch reactors containing Zn64 and sand at various mass ratios. All reactors contained an equal mass load of Zn64. Sand was seen to inhibit TCP degradation to a greater extent when more sand was present.
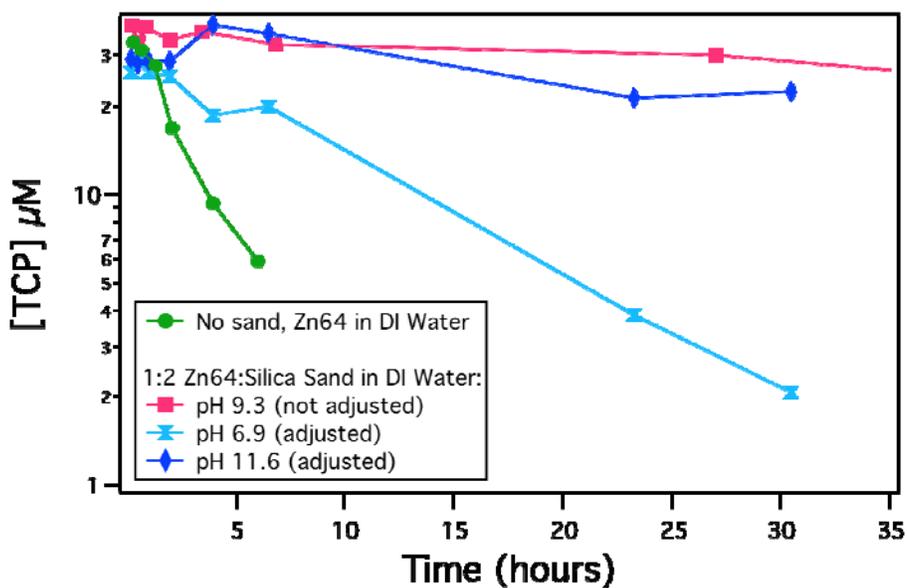
Figure 31. The effect of pH on inhibition by sand in DI water. Batch-reactor experiments were performed with an equal mass of Zn64 and mass ratio of Zn64 to sand but at different pH values. Faster kinetics were observed at pH 6.9 than ph 9.3 or 11.6. This trend is similar to what was observed in batch reactor experiments containing site water.
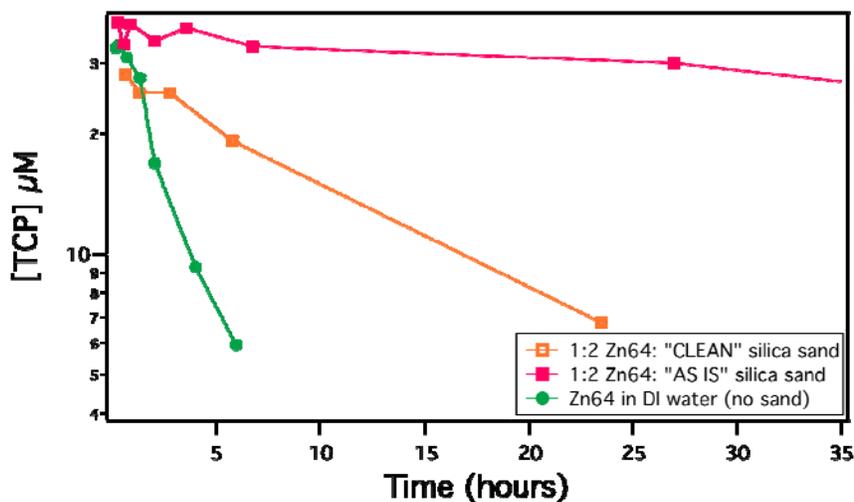
Figure 32. TCP degradation in "clean" vs. "as-is" sand. Batch-reactor experiments containing an equal mass of Zn64 and an equal mass ratio of Zn64 to sand were run. In one case, the sand was used "as-is", in the other case, the sand was cleaned by rinsing a number of times with water. This "clean" sand produced less inhibition of TCP reduction.
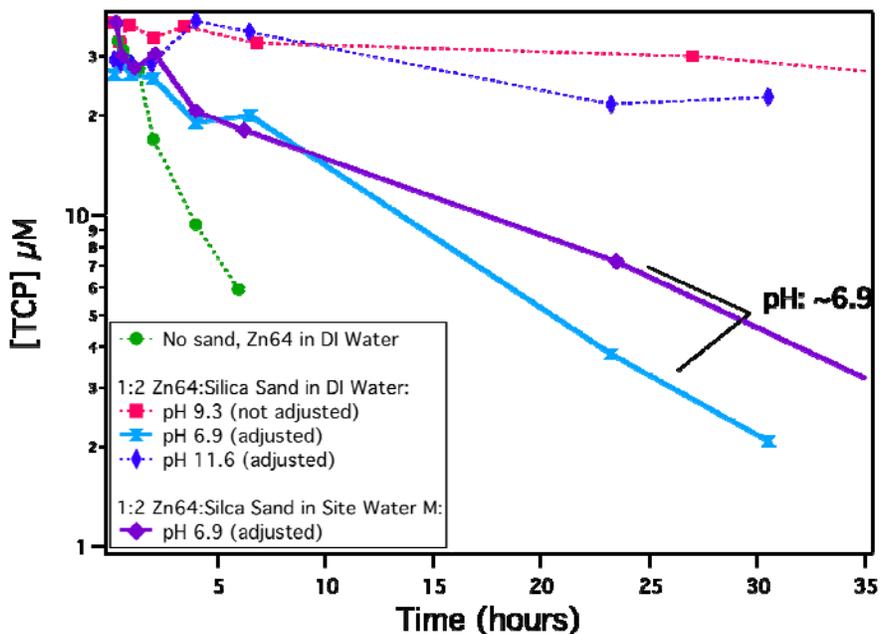
Figure 33. Comparison between batch kinetics of reactors containing ZVZ and sand in DI water and site water at low pH. The curves for 1:2 Zn64:Silica Sand in pH 6.9 DI water and pH 6.9 site water look nearly identical. This result suggests that the inhibition caused by site water and sand are not additive.

Effect of pH

In addition to the effect of groundwater, groundwater solutes, and sand, the effect of pH on TCP degradation was evaluated by performing batch reactor experiments under various pH conditions. pH was varied through the addition of 1N HCl or NaOH 1 hour into a ~24 hr Zn/water pre-equilibration period. Initial pH measurements were made after this equilibration period and prior to TCP injection (reaction initiation).

Two distinct trends were seen in DI water and site water batch experiments. These trends are shown in Figure 34, which plots the observed reaction rate (k_{obs}) vs. batch reactor pH. In DI water experiments, the slowest rates were seen in batch reactors without pH adjustment. The pH of these batches ranged from ~8-10. When the pH was titrated up
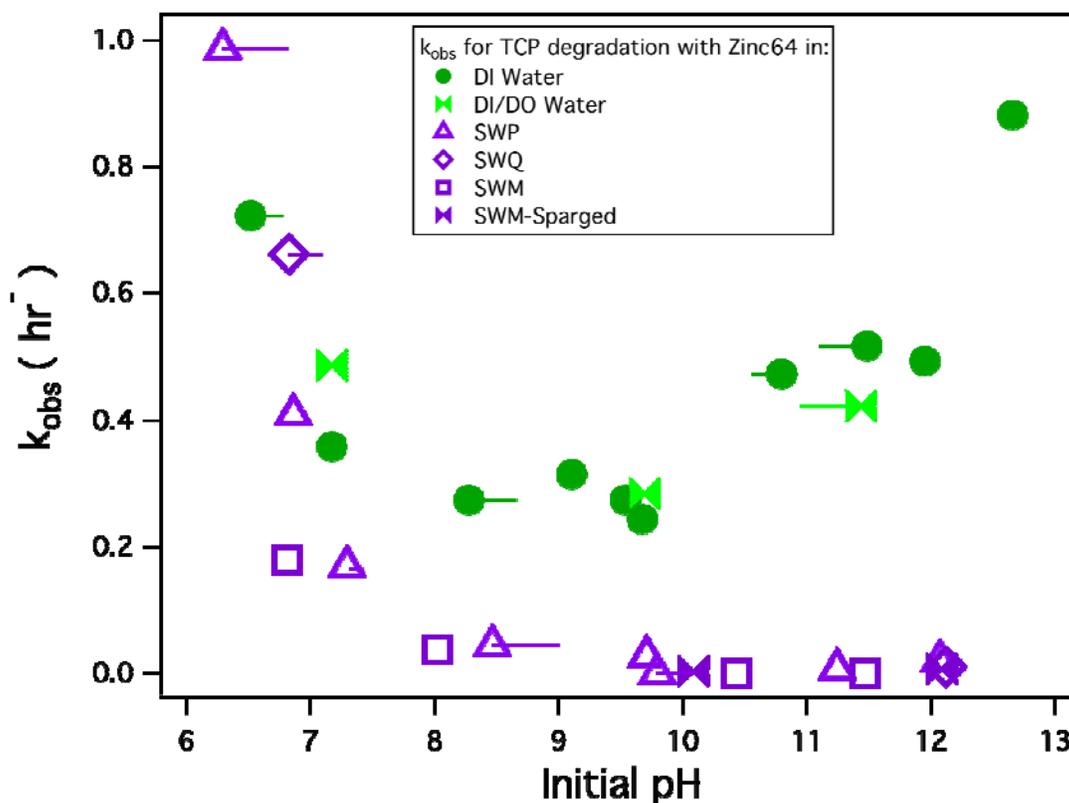
Figure 34. The observed rate of TCP degradation (k_{obs}) by Zn64 versus initial batch reactor pH. Initial pH values were measured after a 24-hour pre-equilibration period but prior to initiation of the reaction though the injection of TCP stock solution. Final pH measurements were taken subsequent to final concentration measurements and are represented here by a line drawn from the initial pH marker to the final pH value; markers shown without this line did not experience a significant shift in pH over the course of the experiment. All reactors contained an equal mass load of Zn64.

or down, k_{obs} increased. This trend matches that of zinc hydroxide solubility. It is possible that the faster kinetics at "extreme" pH values is a result of decreased zinc hydroxide passivation on the ZVZ surface (or at least a change in the surface composition). Hypotheses regarding the trend seen in site water are not as apparent. In site water, there is a general decrease in k_{obs}, except at low pH where site water experiments displayed similar kinetics to DI water experiments. In the case of both DI and site water, sparging the solution prior to the experiment (and preparing the reactor in an oxygen free environment) did not have an effect on the batch kinetics. A similar trend in k_{obs} vs. pH was seen with Zn1210 (Figure 35).
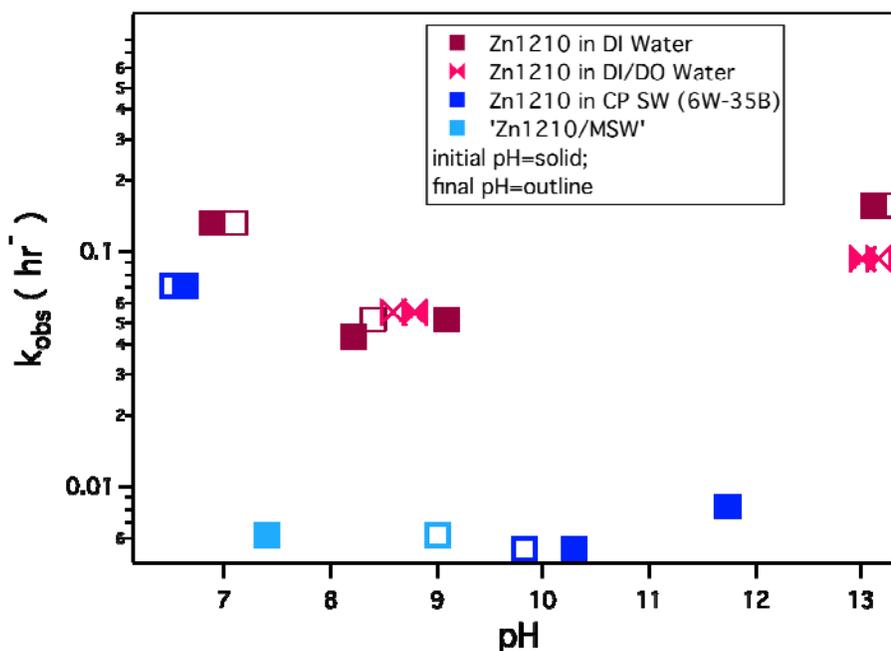
Figure 35. The observed rate of TCP degradation by Zn1210 versus pH. Initial batch reactor pH values are shown by solid symbols, final pH values by hollow symbols. All reactors contained an equal mass load of Zn1210.

Effect of Ionic Strength

In addition to the solution parameters discussed already, the effect of ionic strength on ZVZ reactivity towards TCP was assessed. Initially, results from experiments run under the same conditions of mass, volume, and TCP concentration, but with varying solution chemistries were compared in a QSAR-like fashion to evaluate any effect of ionic strength. Ionic strength was estimated through activity/concentration calculations, so only solutions with known compositions were included (i.e., all DI and AGW solutions were included but site water was not). The results of this exercise are shown in Figure 36. It

appears that, while ionic strength does have an effect on k_{obs}, the effects of silicate, phosphate, and/or pH adjustment predominate.

a)   b)
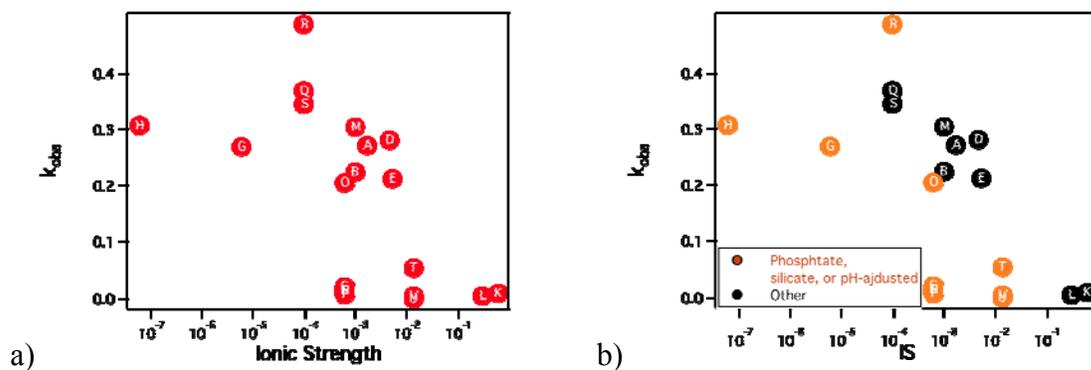
Figure 36. QSAR-type analysis of the effect of ionic strength on reaction rate. (**A**) shows all the data assessed; (**B**) shows the same data, but with solutions that either contained phosphate, silicate, or that had been pH adjusted shown in orange with all other data in black. The trend in (**B**) suggests that, while there is a general ionic strength effect, the presence of phosphate, silicate, or adjustments to batch reactor pH cause deviations that fall outside the general ionic strength trend.

To further identify any effect of ionic strength, batch-reactor experiments were run with varying concentrations of either sodium sulfate ($NaSO_4$) or sodium perchlorate ($NaClO_4$) (results in Figure 37). It was seen that, while ionic strength had a small effect on k_{obs}, it was not large enough to solely explain the inhibition caused by site water.
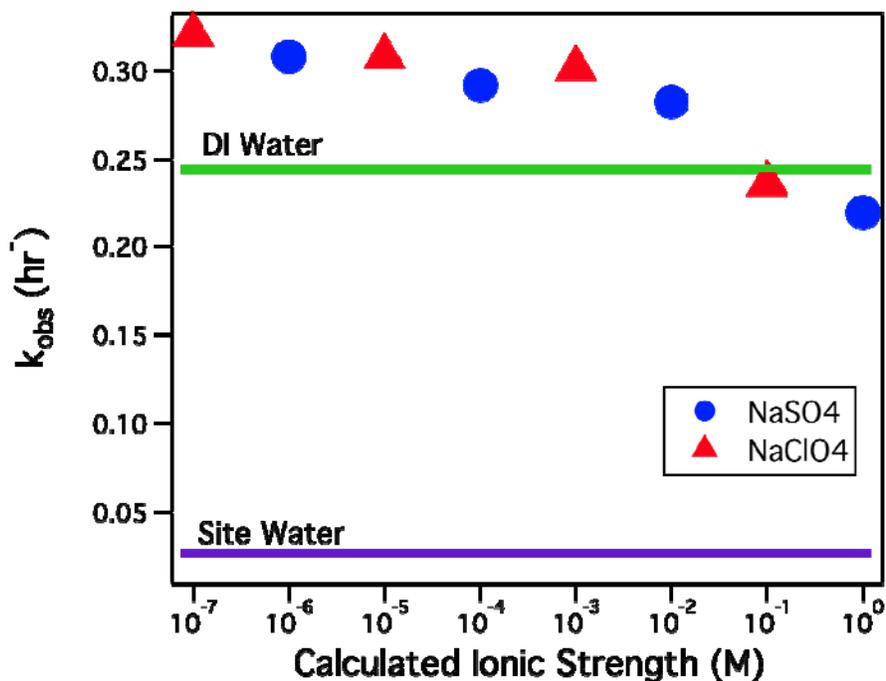
Figure 37. Assessment of the effect of ionic strength by comparison to the reactivity of various batch reactors prepared at a fixed ionic strength. The figure has been annotated with the k_{obs} values measure in DI water and site water as a similar pH for context (note that these lines only represent the k_{obs} value at one ionic strength and not over a range of ionic strengths as might be assumed from the method of figure annotation). All batch reactors were run with the same mass load of Zn64.

Approaches to Overcoming Site Water Inhibition

In addition to pH adjustment, other methods of overcoming site water inhibition were explored. One method was the addition of hydroxyapatite to the batch reactors. This treatment had no apparent effect on site water containing reactors, and in fact inhibited TCP degradation in DI water batches. This inhibition was likely a result of increased phosphate concentrations resulting from hydroxyapatite dissolution. Also explored was treatment with EDTA. This treatment was intended to decrease the amount of zinc hydroxide on the material. While the treatment appeared somewhat successful, large variations in batch reactor pH made the results inconclusive. More recently, zinc columns have been run with a ZVI/iron oxide pre-treatment column, with the hypothesis being that the ZVI column would remove the inhibiting site water constituents. At this time, this treatment has not shown any success.

Task B2. Respike Experiments

Limited, short-term respike experiments were performed. The kinetics of these respike experiments were similar or slightly faster than the initial batch kinetics (results in Figure 38). The kinetics of the respike experiments were either similar to, or faster than the initial kinetics in both DI water and site water. This suggests that ZVZ may not have significant capacity limitations.
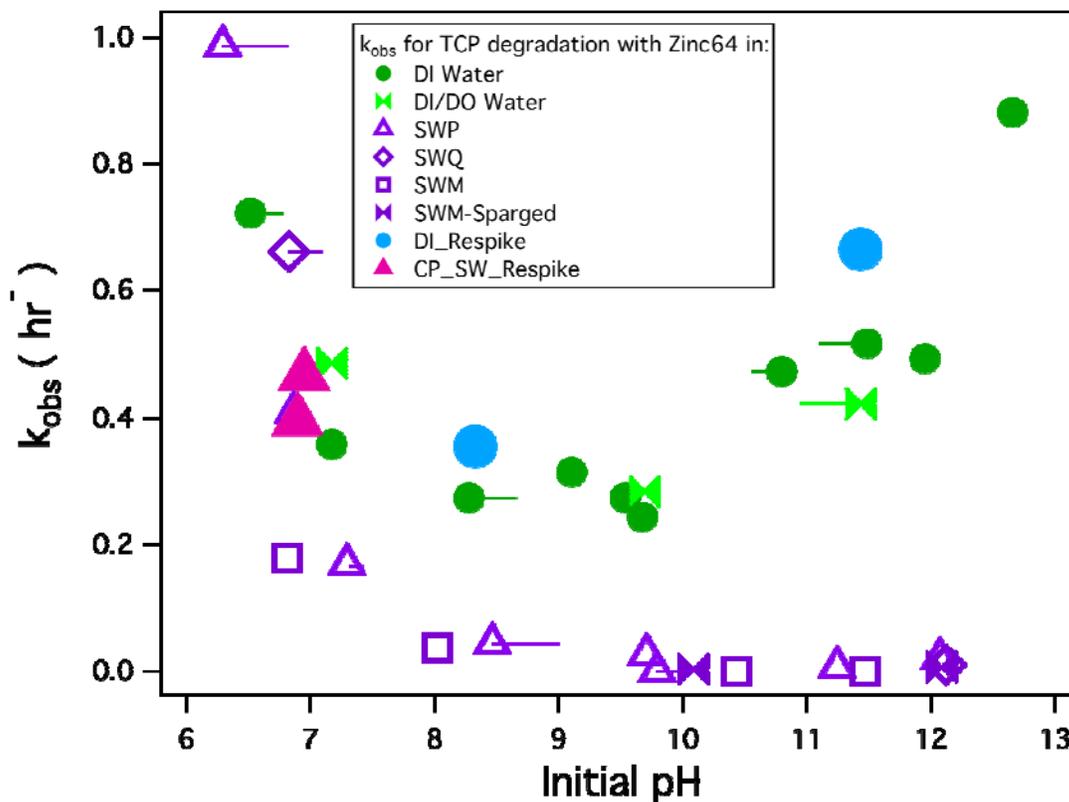
Figure 38. Overlay of respike experiments onto Figure 34. Respikes were separated by about 24 hours.

Task B3. Medium-Term Column Experiments.

Medium-term column experiments were not performed. Short-term column experiments are described below.

Assessing Implications for Water Chemistry and Permeability

Task C1. Column Material/Mixture Optimization

15-cm long, 2.5-cm inner diameter columns were run with different mass percentages of Zn64 in silica sand. The effluent pH was measure over time (Figure 39). The pH of all the columns appeared to be controlled—to the most part—by the sand. Efforts were made to identify a material to replace sand that would buffer the pH at a value below 7 rather than around 8.5. A suitable material was not found.

The concentration of dissolved Zn^{2+} in the column effluent was also measured (Figure 40). The dissolved Zn^{2+} concentration was seen to remain very low at a flow rate of 2 mL/min for Zn64 concentrations in sand of 10% and 20%. At 50% the concentration was much higher, and close to the drinking water limit (5 mg/L).
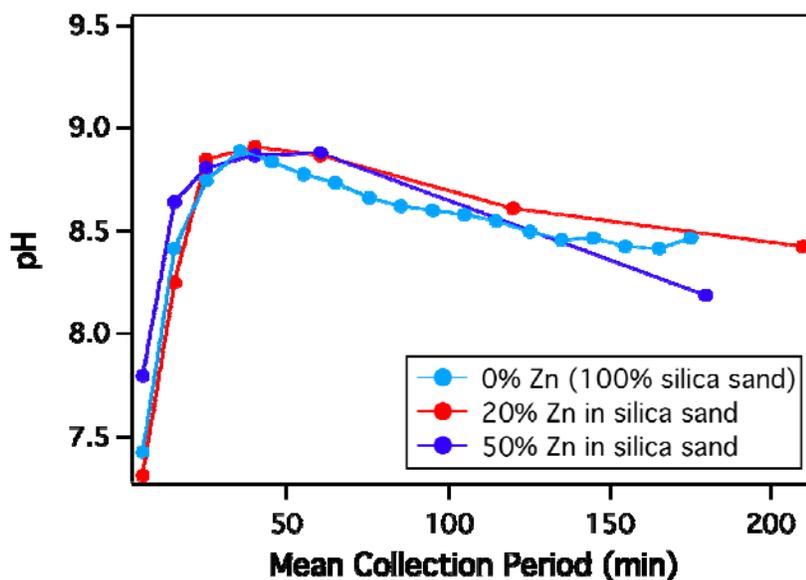
Figure 39. Effect of mass concentration of ZVZ in sand on column effluent pH over time. The pH appears to be independent of ZVZ concentration and therefore controlled by the sand not the ZVZ.
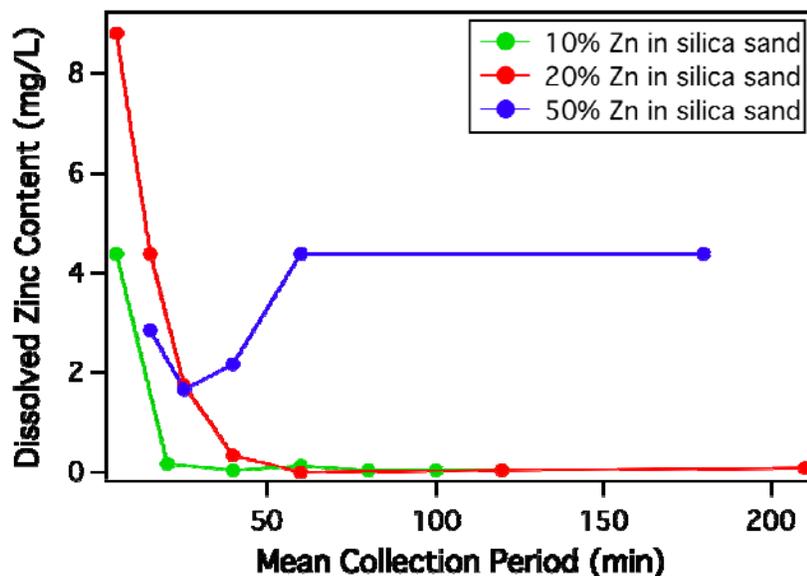
Figure 40. Effect of mass concentration of ZVZ in sand on effluent concentrations of Zn^{2+} over time.

Task C2. Column Performance

15-cm long, 2.5-cm inner diameter columns were run with different packing materials and either DI water or site water[7]. The k_{obs} values obtained from these columns are summarized in Figure 41. Some columns were run with an acidified influent (pH ~2) in an attempt to achieve the faster kinetics observed in acidified batch reactor experiments. The main trends noted were that kinetics were faster in DI water than site water, and faster in acidified site water than site water used without pH adjustment. However, the fast kinetics achieved with acidified influent were not observed in a larger (1m long, 2.2 cm diameter) column (result not shown). It is likely that fast kinetics like those observed in the acidified influent, 15-cm columns only persisted in the first section of the 1-m column (where pH remained low) and did not significantly contribute to the overall k_{obs}.

---

[7] We have published these results in more detail in the Proceedings of the 7th International Conference on Remediation Chlorinated and Recalcitrant Compounds (*20*).
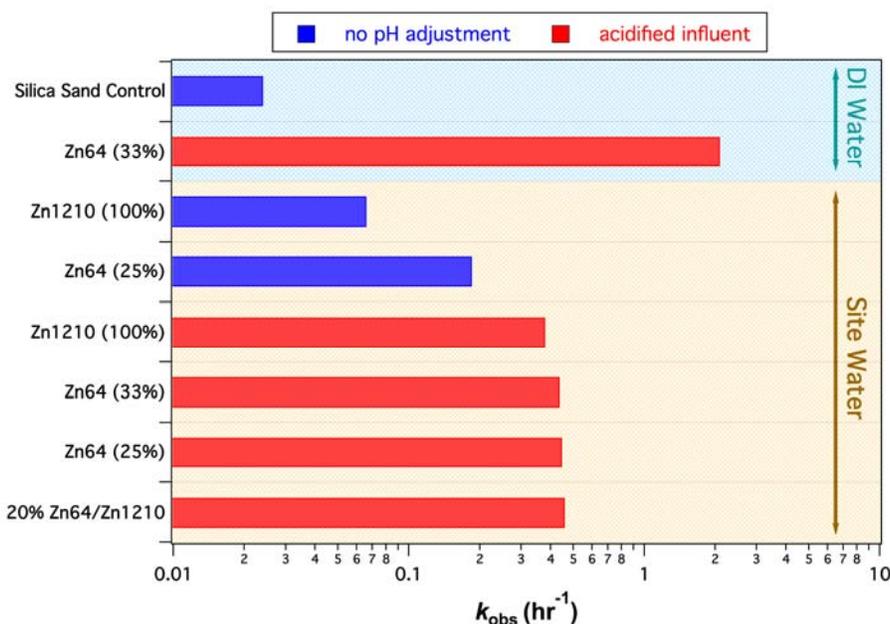
Figure 41. Observed reaction rates for 15-cm long, 2.5-cm inner diameter columns run with various ZVZ materials and various mass concentrations of ZVZ in sand. Column influent was either DI water or site water. In some cases the influent was acidified to a pH of ~2.

Task C3. Geochemical Speciation Modeling

Geochemical speciation modeling is a useful tool for understanding the general behavior and occurrence of solid and dissolved mineral phases in a system. These models rely on a number of assumptions that must be considered, two of which are (*i*) that the model assumes equilibrium, which is unlikely for many natural systems, and (*ii*) that the accuracy of the model is dependent on the accuracy of the thermodynamic constants used in its generation. Despite these caveats, a general understanding of system behavior can still be gained from such exercises and can lead to insight into such parameters as the composition of passivating surface layers.

For this work, geochemical speciation models were created using the ACT subset of the Geochemist's Workbench modeling package (RockWare Inc.) and the thermodynamic constants given in the thermo.com.v8.r6+ dataset. Groundwater diagrams were generated based on the concentrations reported for Site Water P.

Figure 42 shows solubility diagrams generated for Zn^{2+} species in DI water and in groundwater. It can be seen that, in DI water, zincite (ZnO) is the solubility controlling solid. It is likely that ZnO is present on the surface of the ZVZ as a passive layer. This is consistent with the observed trend of increased kinetics at pH values lower and higher than about 8-10—pH values where ZnO is more soluble. A difference in the solubility behavior of the Zn^{2+} species is seen in groundwater. In the groundwater system, zinc silicate (Zn_2SiO_4) replaces ZnO as the controlling solid. More insight into this behavior is

48

given in Figure 43, a predominance diagram for Zn^{2+} species at various concentrations of $SiO_{2(aq)}$. This figure shows that zinc silicate is present, and therefore prescribes (or controls) Zn^{2+} solubility, at $SiO_{2(aq)}$ concentrations higher than $10^{-8.5}$ M or 0.2 ppb (assuming $\gamma = 1$, a typical assumption for neutral species (21)). Typical groundwater concentrations of $SiO_{2(aq)}$ range from 5-85 ppm with a median concentration of 17 ppm (22), suggesting that, as a general rule, zinc silicate will have preferential control over Zn^{2+} species solubility over ZnO in ZVZ groundwater remediation systems. This has consequences for the composition and behavior of any Zn^{2+} solids passivating the surface of the ZVZ. Presumably, the observed inhibited TCP degradation kinetics in groundwater versus DI water are a direct result of passivation with Zn_2SiO_4 instead of ZnO and differences in the solubility and electron permeability of these two mineral phases.

a)   b)
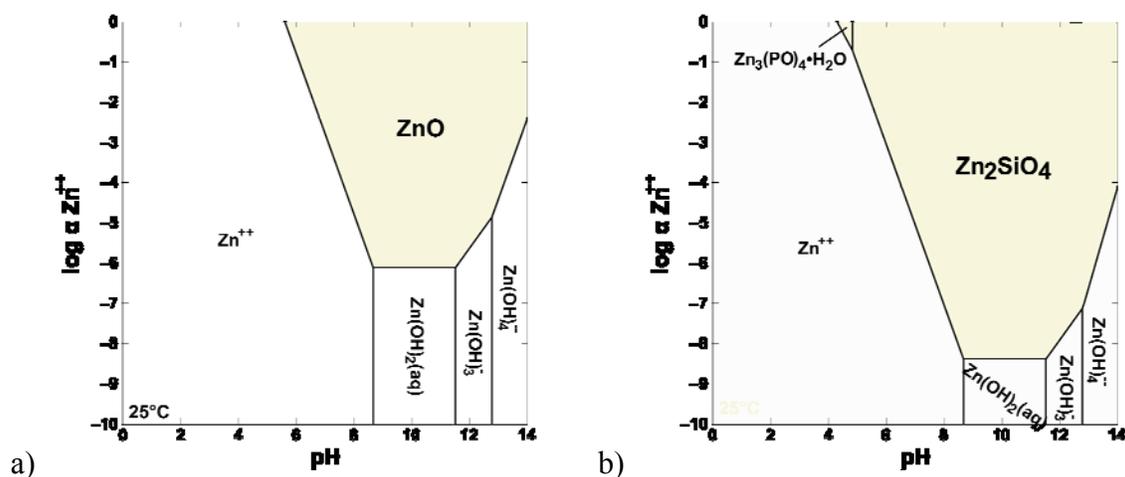
Figure 42. Solubility diagrams for Zn^{2+} species in (**A**) DI water and (**B**) groundwater (Site Water P). Diagrams were generated in Geochemist's Workbench using dataset thermo.com.v8.r6+. Temperature = 25°C; Pressure = 1.013 bars; $\alpha(H_2O) = 1$; all constituent concentrations for (**B**) as reported for Site Water P.
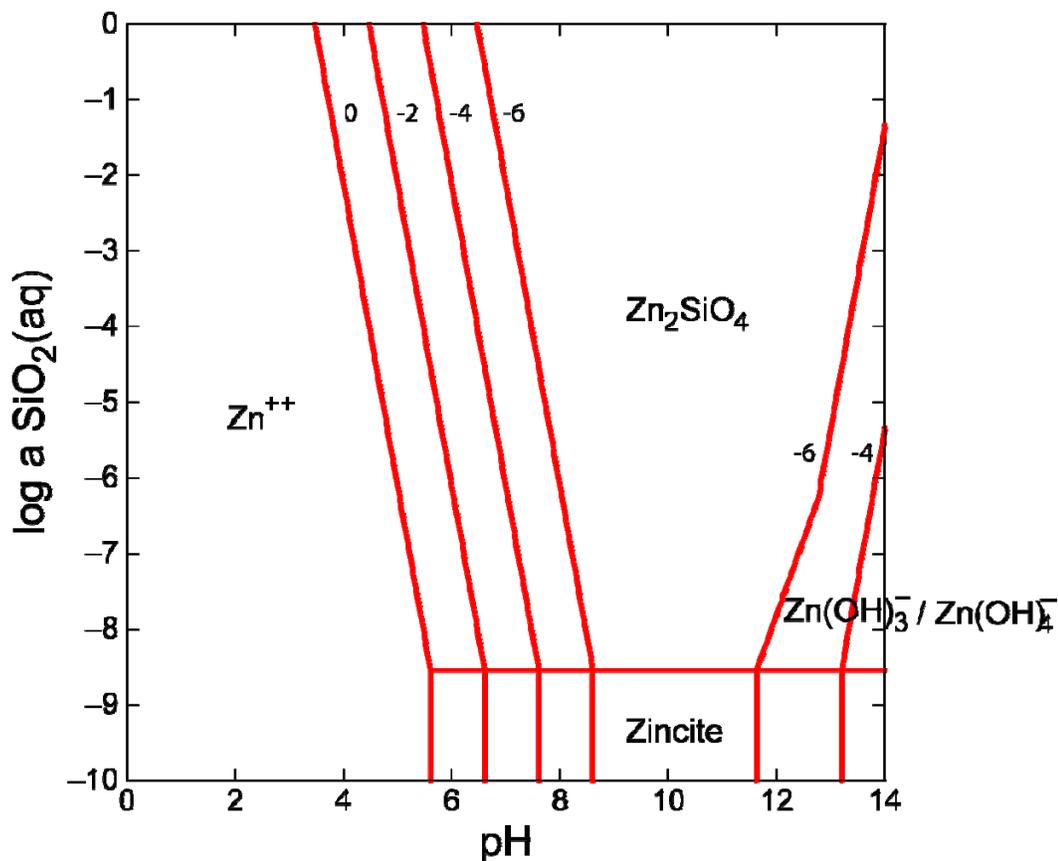
Figure 43. Predominance diagram for Zn^{2+} species in DI water as a function of $SiO_2(aq)$ and pH. Lines shown represent equilibrium species transitions at $[Zn^{2+}]_{Total}$ of 10^0, 10^{-2}, 10^{-4}, 10^{-6}. It can be seen that, at $SiO_2(aq)$ concentrations above $10^{-8.5}$ M (assuming $\gamma = 1$) zinc silicate (Zn_2SiO_4) controls Zn^{2+} species solubility. Below $10^{-8.5}$ M, zincate (ZnO) controls Zn^{2+} species solubility.

Conclusions and Implications

Summary of Specific Conclusions

1. In general, 1,2,3-trichloropropane (TCP) is similarly mobile, exceptionally persistent, and relatively toxic, compared with other chlorinated solvents that occurs as contaminants of groundwater and soil.

2. Available pathways for degradation of TCP include hydrolysis, elimination, reduction, and oxidation. This applies to biotic as well as abiotic transformations of TCP, but the scope of this project included only abiotic processes.

3. Hydrolysis of TCP is slow under environmental conditions, but can be fast at high pH and temperature, and therefore may contribute significantly to attenuation of TCP under conditions of in situ thermal remediation.

4. Oxidation of TCP by mild, selective oxidants like permanganate is negligible.

5. Oxidation of TCP by advanced oxidation processes that involve hydroxyl or sulfate radical (such as activated hydrogen peroxide and activated persulfate) can completely mineralize TCP, but the kinetics are slower than for oxidation of most other organic contaminants.

6. Reduction of TCP is possible, but negligible under conditions relevant to natural attenuation, and slow under conditions of conventional in situ chemical reduction, such as with granular zero-valent iron (ZVI).

7. Stronger reducing systems, such as nano ZVI and palladized ZVI can degrade TCP relatively rapidly, although possibly with accumulation of persistent partial dechlorination products.

8. Reduction of TCP with zero-valent zinc (ZVZ) gave rapid reduction in deionized water, mainly through beta-elimination, to completely dechlorinated products.

9. Industrial-grade ZVZ produces TCP degradation kinetics as fast as those observed with reagent-grade ZVZ.

10. Groundwater inhibits ZVZ reduction of TCP at pH values above about 6.5 or 7.

Implications for Future e Research and Implementation

The approach taken in this project was to do a comprehensive assessment of TCP degradation, covering essentially all of the processes that might contribute to its attenuation in groundwater, whether by natural attenuation or any sort of active remediation. Although some degree of TCP degradation was observed under favorable conditions for hydrolysis, oxidation, and reduction, relatively extreme conditions were needed to obtain significant degradation rates in all cases. Although this study did not investigate any biodegradation processes, the same chemical characteristics that make TCP relatively recalcitrant to abiotic degradation processes also apply to biodegradation processes. This suggests that a highly efficient, targeted process for remediation of TCP is unlikely to be found.

Instead, like other characteristically recalcitrant contaminants, successful resolution of TCP contamination of groundwater will require highly optimized application of existing treatment processes (e.g., activated peroxide or persulfate) or innovative variations on existing processes (e.g., zero-valent zinc instead of zero-valent

iron). Although both of these approaches have promise, considerably more research will be needed before the preferred treatments for TCP contaminated groundwater will become established. This work needs to include—or be closely coordinated with—efforts to manage TCP contamination in the field, because satisfactory solutions must meet requirements across the whole spectrum of considerations.

The challenge of evaluating the overall suitability of a TCP remediation process is particularly acute with regard to the use of granular ZVZ, because ZVZ has not been used in field scale groundwater remediation previously. Although initial results obtained in the laboratory were very promising, follow-up testing with water from field sites were less promising, due to site water chemistry effects that seem to be larger than expected based on experience with ZVI. More experience with ZVZ over a range of conditions will be needed before the overall significance of these results can be assessed.

References

(1)   Kielhorn, J.; Könnecker, G.; Pohlenz-Michel, C.; Schmidt, S.; Mangelsdorf, I. 1,2,3-Trichloropropane, World Health Organization, Geneva, 2003.

(2)   National Toxicology Program 11th Report on Carcinogens. In U.S. Department of Health and Human Services, Public Health Service, National Institutes of Health, Bethesda, MD: 2005.

(3)   Tratnyek, P. G.; Sarathy, V.; Fortuna, J. H., Fate and remediation of 1,2,3-trichloropropane. In International Conference on Remediation of Chlorinated and Recalcitrant Compounds, 6th, Monterey, CA, 2008, Vol. pp. Paper C-047.

(4)   Sarathy, V.; Tratnyek, P. G.; Salter, A. J.; Nurmi, J. T.; Johnson, R. L.; Johnson, G. O. B. Degradation of 1,2,3-trichloropropane (TCP): Hydrolysis, elimination, and reduction by iron and zinc. Environ. Sci. Technol. 2010, 44, 787-793.

(5)   Ellington, J. J.; Stancil, F. E.; Payne, W. D. Measurement of hydrolysis rate constants for evaluation of hazardous waste land disposal. Volume 1. Data on 32 chemicals, U.S. Environmental Protection Agency. 1986.

(6)   Pagan, M.; Cooper, W. J.; Joens, J. A. Kinetic studies of the homogeneous abiotic reactions of several chlorinated aliphatic compounds in aqueous solution. Applied Geochemistry 1998, 13, 779-785.

(7)   Focht, R. M.; Gillham, R. W. Dechlorination of 1,2,3-Trichloropropane by zero-valent iron, Preprint Extended Abstracts. In 209th ACS National Meeting; American Chemical Society, Division of Environmental Chemistry: Anaheim, CA, 1995, 35, No. 1, pp. 741-744.

(8)   Scherer, M. M.; Balko, B. A.; Gallagher, D. A.; Tratnyek, P. G. Correlation analysis of rate constants for dechlorination by zero-valent iron. Environ. Sci. Technol. 1998, 32, 3026-3033.

(9)   Klausen, J.; Vikesland, P. J.; Kohn, T.; Burris, D. R.; Ball, W. P.; Roberts, A. L. Longevity of granular iron in groundwater treatment processes: solution composition effects on reduction of organohalides and nitroaromatic compounds. Environ. Sci. Technol. 2003, 37, 1208-1218.

(10)   Focht, M. R. Bench-Scale Treatability Testing to Evaluate the Applicability of Metallic Iron for Above-Ground Remediation of 1,2,3-Trichloropropane Contaminated Groundwater. Thesis, University of Waterloo, 1994.

(11)   Nurmi, J. T.; Tratnyek, P. G.; Sarathy, V.; Baer, D. R.; Amonette, J. E.; Pecher, K.; Wang, C.; Linehan, J. C.; Matson, D. W.; Penn, R. L.; Driessen, M. D.

Characterization and properties of metallic iron nanoparticles: Spectroscopy, electrochemistry, and kinetics. Environ. Sci. Technol. 2005, 39, 1221-1230.

(12) Sarathy, V.; Tratnyek, P. G.; Nurmi, J. T.; Baer, D. R.; Amonette, J. E.; Chun, C.; Penn, R. L.; Reardon, E. J. Aging of iron nanoparticles in aqueous solution: effects on structure and reactivity. J. Phys. Chem. C 2008, 112, 2286-2293.

(13) Wang, C.-B.; Zhang, W.-X. Synthesizing nanoscale iron particles for rapid and complete dechlorination of TCE and PCBs. Environ. Sci. Technol. 1997, 31, 2154-2156.

(14) Song, H.; Carraway, E. R. Reduction of chlorinated ethanes by nanosized zero-valent iron: Kinetics, pathways, and effects of reaction conditions. Environ. Sci. Technol. 2005, 39, 6237-6245.

(15) Bylaska, E. J.; Glaesemann, K. R.; Felmy, A. R.; Vasiliu, M.; Dixon, D. A.; Tratnyek, P. G. Free energies for degradation reactions of 1,2,3-trichloropropane from ab initio electronic structure theory. J. Phys. Chem. A 2010, submitted.

(16) Arnold, W. A.; Ball, W. P.; Roberts, A. L. Polychlorinated ethane reaction with zero-valent zinc: Pathways and rate control. J. Contam. Hydrol. 1999, 40, 183-200.

(17) Nurmi, J. T.; Tratnyek, P. G. Electrochemical studies of packed iron powder electrodes: Effects of common constituents of natural waters on corrosion potential. Corros. Sci. 2008, 50, 144-154.

(18) Hunter, F. Fenton's treatment of 1,2,3-trichloropropane: chemical reaction byproducts, pathways, and kinetics. In Proceedings of the International Symposium on Chemical Oxidation: Technology for the Nineties; Technomic, 1997; Vol. 6; pp. 50-71.

(19) Hoigné, J. The chemistry of ozone in water. In Process Technologies for Water Treatment; Plenum, 1988; pp. 121-143.

(20) Salter, A. J.; Johnson, R. L.; Tratnyek Paul, G., Degradation of 1,2,3-trichloropropane by zero-valent zinc: Laboratory assessment for field application. In International Conference on Remediation of Chlorinated and Recalcitrant Compounds, 7th, Monterey, CA, 2010, in press.

(21) Pankow, J. F. Aquatic Chemistry Concepts; CRC Press: Boca Raton, 1991.

(22) Langmuir, D. Aqueous Environmental Geochemistry; Prentice-Hall, Inc.: Upper Saddle River, NJ, 1997.

Appendices

Presentations

Paul G. Tratnyek, Vaishnavi Sarathy, Patty Toccalino (2005) 1,2,3-Trichloropropane: Occurrence, Fate, Causes for Concern, and Remediation through Abiotic Pathways. International Chemical Congress of Pacific Basin Societies (Pacifichem) 15-20 December 2005, Honolulu, HI.

Sarathy, V. and P. G. Tratnyek. 2006. 1,2,3-Trichloropropane (TCP): Occurrence, Fate, and Risk.. 5th International Conference on Remediation of Chlorinated and Recalcitrant Compounds, Monterey, CA, 22-25 May 2006. (poster)

Paul G. Tratnyek, Vaishnavi Sarathy, Rachel Waldemer, Syeda Ahmed. (2006) 1,2,3-Trichloropropane: Occurrence, Fate, Remediation, and Risk; Workshop on Emerging Contaminants in Groundwater, California Groundwater Resources Association, 7-8 June 2006, Concord, CA.

Paul G. Tratnyek and Vaishnavi Sarathy (2008) Fate and Remediation of 1,2,3-Trichloropropane. 6th Annual Conference on Remediation of Chlorinated and Recalcitrant, 19-22 May 2008, Monterey, CA.

Paul G. Tratnyek, Vaishnavi Sarathy, James T. Nurmi, Graham O'Brien Johnson, and Rick Johnson (2008) Prospects for Remediation of 1,2,3-Trichloropropane (TCP); Workshop on Emerging Contaminants in Groundwater, California Groundwater Resources Association, 19-20 November 2008, San Jose, CA.

Salter, A. J., P. G. Tratnyek, J. T. Nurmi. 2009. Prospects for remediation of the emerging contaminant 1,2,3-trichloropropane using zero-valent zinc. 68th Oregon Academy of Science Annual Meeting, 28 February 2009, Monmouth, OR.

Salter, Alexandra J.; Johnson, Richard L.; Paul G. Tratnyek. Degradation of 1,2,3-trichloropropane by zero-valent zinc: Laboratory assessment for field application. 6th Annual Conference on Remediation of Chlorinated and Recalcitrant Compounds, 23-27 May 2010, Monterey, CA.

Publications

Vaishnavi Sarathy (**2008**) Engineered Remediation and Natural Attenuation of Halogenated Alkanes (Carbon Tetrachloride and 1,2,3-Trichloropropane): A Study of Contaminant Reactivity and Reductant Morphology. Oregon Health & Science University, Ph.D. Thesis.

Tratnyek, P. G., V. Sarathy, and J. H. Fortuna, **2008**, Fate and remediation of 1,2,3-trichloropropane, In Proceedings of the International Conference on Remediation of

Chlorinated and Recalcitrant Compounds, 6th International Conference on Remediation of Chlorinated and Recalcitrant Compounds, 6th, Monterey, CA.

Sarathy, Vaishnavi; Tratnyek, Paul G.; Salter, Alexandra J.; Nurmi, James T.; Johnson, Richard L.; O'Brien Johnson, Graham. Degradation of 1,2,3-trichloropropane (TCP): Hydrolysis, elimination, and reduction by iron and zinc. *Environ. Sci. Technol.* **2010**, *44*, 787-793.

Tratnyek, P. G.; Salter, Alexandra J.; Nurmi, James T.; Sarathy, Vaishnavi. Environmental applications of zerovalent metals: Iron vs. zinc. In *Nanoscale Materials in Chemistry: Environmental Applications*; Erickson, L. E.; Koodali, R. T.; Richards, R. M., Eds.; American Chemical Society, **2010**, in press.

Salter, Alexandra J.; Johnson, Richard L.; Tratnyek, Paul G., Degradation of 1,2,3-trichloropropane by zero-valent zinc: Laboratory assessment for field application. In *International Conference on Remediation of Chlorinated and Recalcitrant Compounds, 7th,* Monterey, CA, **2010**, in press.

Salter-Blanc, Alexandra; Tratnyek, Paul G. **2010**. The effect of solutes on the degradation of 1,2,3-trichloropropane by zero-valent zinc. In preparation.